1964

Sound dispersion in binary mixtures of halomethane gases

Rodney Russett Boade
Iowa State University

SOUND DISPERSION IN BINARY MIXTURES OF HALOMETHANE GASES

by

Rodney Russett Boade

A Dissertation Submitted to the
Graduate Faculty in Partial Fulfillment of
The Requirements for the Degree of
DOCTOR OF PHILOSOPHY

Major Subject: Physics

Approved:

Signature was redacted for privacy.

In Charge of Major Work

Signature was redacted for privacy.

Head of Major Department

Signature was redacted for privacy.

Dean of Graduate College

Iowa State University
Of Science and Technology
Ames, Iowa

1964

TABLE OF CONTENTS

I. INTRODUCTION

The phenomena of sound dispersion in polyatomic gases, i.e. the dependence of the velocity of sound on frequency, was first observed by Pierce (22) in 1925. Using a piezoelectric crystal as a sound source, he measured the velocity of sound in carbon dioxide at various frequencies. At about 100 kilocycles per second he observed that the sound velocity increased with increasing frequency. This was in direct conflict with the classical theory of sound propagation which predicts no dependence of velocity on frequency.

This discrepancy can be explained by considering the various degrees of freedom of a polyatomic molecule and assuming that molecular collisions are responsible for the exchange of energy between these degrees of freedom. At ordinary temperatures the energy of a molecule is made up of contributions from the translational, rotational, and vibrational degrees of freedom. The electronic contribution is negligible. The classical theory of sound propagation is based on an assumption that all these degrees of freedom remain in thermal equilibrium throughout the acoustic cycle. This is true at low frequencies. However, at high frequencies the internal degrees of freedom (vibrational, rotational) do not remain in thermal equilibrium and are said to lag the acoustic cycle. This is due to

the inefficiency of molecular collisions in transferring energy between the internal and external degrees of freedom. For halo-methane gases, from about 100 to about 10,000 (2, 27) collisions are necessary before a quantum of vibrational energy is transferred to translational energy. Therefore, at high frequencies the time between acoustic excitations becomes so short that the prescribed number of collisions no longer occurs and a condition of thermal equilibrium no longer exists. The specific heat associated with the internal degrees of freedom, consequently, no longer contributes to the total specific heat and one observes an increase in the sound velocity.

The vibrational degrees of freedom are the first to lag the acoustic cycle as the frequency is increased. For halo-methane gases this occurs at frequencies from about 0.1 megacycles per second to about 100 megacycles per second. At much higher frequencies the rotational degrees of freedom have also been observed to lag the acoustic cycle.[1] This would indicate that molecular collisions are much more efficient in transferring energy between rotational and translational degrees of freedom than between vibrational and translational. Throughout the remainder of this discussion we will be concerned only with the inability of the vibrational degrees of freedom to remain in thermal equilibrium.

In the years following Pierce's discovery, much effort was expended in the study of sound dispersion in light diatomic and triatomic molecules. In more recent years the study of heavy, more complex molecules has come into prominence (2, 8, 19, 29, 32) along with increased interest in gas mixtures (1, 21, 35). The important quantity obtained from studies of this nature is the vibrational relaxation time of the gas or gas mixture in question. This quantity is a time characterizing the rate at which thermal equilibrium is re-established after the vibrational modes of a gas have been disturbed from their equilibrium value. It is defined as the time required for the departure from equilibrium to decrease to 1/e of its initial value, where e is the base of natural logrithms. As will be seen later, the relaxation time can be used to determine the probability of energy transfer between the translational and vibrational degrees of freedom. The probability of energy transfer is itself a function of the intermolecular potential, so information useful in determining a correct intermolecular force law can be obtained. Gas mixture studies also provide information useful in determining the dependence of the relaxation times of the mixture on the individual relaxation times of the component gases.

Through the years several theories have been presented to predict the probability of energy transfer during a

molecular collision. An important contribution to the understanding of energy transfer was made by Landau and Teller in 1936 (17). They used classical methods and showed that the probability of energy transfer depends strongly on the degree to which the transition process is adiabatic. Their work, however, resulted only in the correct temperature dependence of the relaxation time since lack of knowledge pertaining to parameters in their intermolecular potential function prevented them from calculating any absolute values.

Prior to Landau and Teller's work, several theories of questionable value were presented. Kallmann and London (15), Rice (25), and Zener (37) gave quantum mechanical treatments of the problem. Zener (36) also gave a classical approach. In all these works the interaction potential used was far from the actual one existing, and as a result they were able to show only that collisions were considerably more effective in transferring rotational energy than vibrational energy.

In more recent times, Schwartz, Slawsky, and Herzfeld (31); Schwartz and Herzfeld (30); and several others (3, 6, 21, 33) have applied the principles of Landau and Teller to a more realistic potential and have achieved some success in predicting values for relaxation times. These theories, along with Landau and Teller's, are presented in

some detail later in this work.

The work reported here is concerned with binary mixtures of several halo-methane gases. All possible binary combinations of CH_2F_2, CHF_3, CF_4, CCl_2F_2 and $CHCl_2F$ have been examined. The relaxation times of these mixtures have been determined as a function of concentration. Existing theories have been extended to apply to mixtures of this type. The experimental relaxation times have been compared with those calculated from the theory.

II. THEORY

A. Classical Sound Propagation

The equation

$$V^2 = \left(\frac{\partial P}{\partial \rho}\right)_T + \frac{MT}{\rho^2 C}\left(\frac{\partial P}{\partial T}\right)_\rho^2 \qquad \text{(Eq. 1)}$$

for the velocity of sound has been derived by Richards (26) for a low amplitude, plane sound wave traveling in an isotropic, homogeneous fluid medium. Here, V is the velocity of the sound wave, P is the pressure, ρ is the density, T is the absolute temperature, M is the molecular weight, and C is the specific heat at constant volume. (Throughout this discussion all specific heats will be at constant volume unless otherwise specified.) Richards assumed that the sound wave was transmitted adiabatically, which is apparently quite true for low amplitude waves, since his results agree very well with experimentally determined velocities.

For an ideal gas, i.e. one whose equation of state is given by

$$P = \frac{\rho}{M} RT \ , \qquad \text{(Eq. 2)}$$

where R is the universal gas constant, Equation 1 becomes

$$V^2 = \frac{RT}{M}\left(1 + \frac{R}{C}\right) . \qquad \text{(Eq. 3)}$$

B. Dispersion Theory

1. General discussion

At low frequencies the specific heat of a polyatomic gas is given by

$$C_o = C_{tr} + C_{rot} + C_{vib} , \qquad \text{(Eq. 4)}$$

where C_{tr}, C_{rot}, and C_{vib} are the translational, rotational, and vibrational contributions to the specific heat, respectively. As the frequency of the sound wave increases, C_{vib} is no longer effective and the specific heat becomes

$$C_\infty = C_o - C_{vib} = C_{tr} + C_{rot} . \qquad \text{(Eq. 5)}$$

The subscripts on C_o and C_∞ indicate values of C below and above the dispersive region respectively and correspond to the low and high frequency specific heats respectively. The velocity equation then becomes

$$V_o^2 = \frac{RT}{M}\left(1 + \frac{R}{C_o}\right) \qquad \text{(Eq. 6a)}$$

and

$$V_\infty^2 = \frac{RT}{M}\left(1 + \frac{R}{C_\infty}\right) \qquad \text{(Eq. 6b)}$$

for frequencies below and above the dispersive region, respectively.

At intermediate frequencies the fact that the velocity is a function of frequency is a consequence of the specific heat being a function of frequency. If we replace the specific heat, C, in Equation 3 by

$$C = C(\omega) = C_\infty + \frac{C_{vib}}{1 + i\omega\tau}\ , \qquad \text{(Eq. 7)}$$

we have the following complex expression for V^2,

$$V_\omega^2 = \frac{RT}{M}\left(1 + R\,\frac{1 + i\omega\tau}{C_\infty + C_{vib} + i\omega\tau C_\infty}\right)$$

$$= \frac{RT}{M}\left(1 + R\,\frac{1 + i\omega\tau}{C_o + i\omega\tau C_\infty}\right)\ . \qquad \text{(Eq. 8)}$$

Here ω is $2\pi f$, τ is the relaxation time and f is the frequency. Taking the real part we have

$$\mathcal{R}e\ V_\omega^2 = \frac{RT}{M}\left(1 + R\,\frac{C_o + \omega^2\tau^2 C_\infty}{C_o^2 + \omega^2\tau^2 C_\infty^2}\right) , \qquad \text{(Eq. 9)}$$

which is an expression for the sound velocity valid throughout the entire frequency range. In the limit of low frequencies Equation 9 reduces to Equation 6a and in the limit of high frequencies to Equation 6b.

A convenient method for obtaining the relaxation time from velocity data is to plot V^2 vs. log(f). Differentiating Equation 9 with respect to log(f) twice and setting the result equal to zero, one finds the inflection frequency, denoted by f_i, of Equation 9 to occur at

$$f_i = \frac{1}{2\pi\tau}\,\frac{C_o}{C_\infty} . \qquad \text{(Eq. 10)}$$

V^2 at this point is

$$V_i^2 = \frac{V_\infty^2 + V_o^2}{2} . \qquad \text{(Eq. 11)}$$

Thus, if one finds the inflection frequency experimentally, the relaxation time can be determined.

When considering polyatomic molecules with several normal modes of vibration, it is reasonable to expect there will be a relaxation time associated with each mode. In most cases, however, this is not observed. It has been

conjectured that the vibrational degrees of freedom of a molecule are strongly coupled together, permitting energy transfers within a molecule, and that transfers of energy between internal and external degrees of freedom take place only through the mode of lowest frequency, known as the exchange mode. That is to say, in de-excitation, the energy of a higher mode is first transferred to the exchange mode and then to the external degrees of freedom. This then implies relaxation times for the internal energy transitions. These relaxation times are evidently so short they are not observed. Since the internal states of a molecule are states of definite energy, these internal transitions can take place only during a collision in order that the energy differences of the internal states may be compensated for by some energy transfer to the external degrees of freedom. This is known as excitation in series.

In some molecules the intermodal coupling breaks down. In such cases, the concept of parallel excitation is employed. This means that the frequency dependent specific heat is written as

$$C(\omega) = C_{\infty} + \sum_{j} \frac{C_j}{1 + i\omega\tau_j} , \qquad \text{(Eq. 12)}$$

where τ_j is the relaxation time of the j^{th} energy transfer

and C_j is the specific heat associated with it. C_2H_6 (34) and CH_2Cl_2 (32), which both exhibit two relaxation times, are examples of gases which behave in this manner. The apparent reason for this behavior is a large gap in the vibrational spectra of these gases. For the case where j has two values in Equation 12 one obtains for V^2 (34),

$$V_\omega^2 = \frac{RT}{M}\left(1 + R\,\frac{C_o + \omega^2 A + \omega^4 B}{C_o^2 + \omega^2 D + \omega^4 E}\right) , \qquad \text{(Eq. 13)}$$

where

$$A = C_\infty \tau_1^2 + C_2 \tau_1^2 + C_\infty \tau_2^2 + C_1 \tau_2^2 ,$$

$$B = C_\infty \tau_1^2 \tau_2^2 ,$$

$$D = C_\infty^2 \tau_1^2 + C_\infty^2 \tau_2^2 + 2C_\infty C_2 \tau_1^2$$

$$+ C_2^2 \tau_1^2 + 2C_\infty C_1 \tau_2^2 + C_1^2 \tau_2^2 + 2C_1 C_2 \tau_1 \tau_2 ,$$

and

$$E = C_\infty^2 \tau_1^2 \tau_2^2 .$$

The quantity of theoretical interest is the relaxation time of the exchange vibrational mode. For a gas whose entire vibrational energy is transferred through one exchange mode this quantity is given by

$$\tau_m = \frac{C_m}{C_{vib}} \tau \ , \qquad \text{(Eq. 14)}$$

where C_m is the specific heat associated with the exchange mode. Where more than one relaxation time is observed the C_{vib} is replaced by the total specific heat of the modes relaxing through each exchange mode.

2. Application to mixtures

The equations developed above can be used for mixtures if the quantities pertinent to the individual gases are replaced by effective quantities for the mixture. Let us consider a binary mixture of gas A and gas B. The mole fractions of gas A and gas B are X and (1 - X) respectively. The effective quantities to be used are as follows:

$$\begin{aligned} M_{eff} &= M_A X + M_B(1 - X) \ , \\ (C_o)_{eff} &= C_{oA} X + C_{oB}(1 - X) \ , \\ (C_\infty)_{eff} &= C_{\infty A} X + C_{\infty B}(1 - X) \ , \end{aligned} \qquad \text{(Eq. 15)}$$

and

$$(C_{vib})_{eff} = (C_{vib})_A X + (C_{vib})_B (1 - X) \ .$$

The frequency dependent specific heat for the mixture, assuming a single relaxation time, is

$$C(\omega)_{eff} = (C_\infty)_{eff} + \frac{(C_{vib})_{eff}}{1 + i\omega\tau} \qquad \text{(Eq. 16)}$$

and results in a velocity equation given by

$$V_\omega^2 = \frac{RT}{M_{eff}} \left[1 + R \frac{(C_o)_{eff} + \omega^2\tau^2(C_\infty)_{eff}}{(C_o)_{eff}^2 + \omega^2\tau^2(C_\infty)_{eff}^2}\right] . \qquad \text{(Eq. 17)}$$

The observed relaxation time then is

$$\tau = \frac{1}{2\pi f_i} \frac{(C_o)_{eff}}{(C_\infty)_{eff}} . \qquad \text{(Eq. 18)}$$

The case of multiple relaxation will be discussed later as will the dependence of the relaxation time of the mixture on the relaxation times of individual mixture constituents.

C. Specific Heats

The gases discussed here are all non-linear polyatomic gases. Therefore, by the equipartition of energy principle, the specific heat associated with translation and rotation is given by 3R. The vibrational specific heats can be calculated to sufficient accuracy at room

temperatures by using the Planck-Einstein equation (16),

$$C_{vib} = \sum_j \frac{q_j (\frac{h\nu_j}{kT})^2 R}{2[\cosh(\frac{h\nu_j}{kT}) - 1]} . \qquad \text{(Eq. 19)}$$

Here h is Planck's constant, k is Boltzmann's constant, ν_j is the frequency of the j^{th} vibrational mode, and q_j is the degeneracy of the j^{th} mode. The vibrational spectra of the gases examined in this study are listed in Table 1 in wave number notation, i.e. in units of $\bar{\nu}_j = \nu_j/c$ where c is the velocity of light.

Table 1. Molecular vibrational spectra in cm^{-1}

CH_2F_2(23)[a]	CHF_3(9)	CF_4(11)	CCl_2F_2(4)	$CHCl_2F$(9)
532	508(2)[b]	437(2)	260	274
1078	697	630(3)	320	366
1089	937(2)	904	433	454
1170	1117	1265(3)	455	723
1262	1376(2)		669	786
1435	3062		885	1065
1508			920	1250
2963			1095	1307
3030			1155	3019

[a]Indicates reference.

[b]Indicates degeneracy.

D. Ideal Corrections

The equations developed in the previous sections are valid only for ideal gases. Since the behavior of the gases examined here deviates considerably from ideal behavior, it is necessary to correct for such deviations. Sette *et al.* (32), using the viral equation of state, have obtained the following correction term valid to first order in P:

$$\frac{V_r}{V_i} = 1 - \alpha P \ . \qquad \text{(Eq. 20)}$$

Here V_r is the velocity in the real gas, V_i is the corrected velocity and α is given by

$$\alpha = - \left[\frac{B}{RT} + \frac{1}{C_o}\left(\frac{dB}{dT} + \frac{RT}{2C_o^P}\frac{d^2B}{dT^2}\right)\right] , \qquad \text{(Eq. 21)}$$

where B is the second viral coefficient and C_o^P is the specific heat at constant pressure at low frequencies. For dilute gases, B can be obtained from the critical temperature, T_c, and the critical pressure, P_c, by using the Berthelot relation (13),

$$B = \frac{9}{128}\frac{RT_c}{P_c}\left(1 - 6\frac{T_c^2}{T^2}\right) \ . \qquad \text{(Eq. 22)}$$

Taking the proper derivatives of B and substituting into Equation 21 one obtains

$$\alpha = -\frac{9}{128}\frac{T_c}{P_c T}\left[1 + 6\frac{T_c^2}{T^2}\left(\frac{2R}{C_o} - \frac{3R^2}{C_o^P C_o} - 1\right)\right] . \qquad \text{(Eq. 23)}$$

When mixtures are being considered effective values for C_o, C_o^P, T_c, and P_c must be used and are given by Equation 15 and by

$$(C_o^P)_{eff} = (C_{oA}^P)X + (C_{oB}^P)(1 - X) ,$$

$$(T_c)_{eff} = T_{cA}X + T_{cB}(1 - X) , \qquad \text{(Eq. 24)}$$

and

$$(P_c)_{eff} = P_{cA}X + P_{cB}(1 - X) .$$

E. Relaxation Theory

In general the equations governing the transfer of energy from one state to another are reaction rate equations. There will be such an equation for each energy state and the question is, how can these equations be combined to give a single equation for the whole internal energy? Two cases, one with two energy states, and the

other a simple harmonic oscillator with an infinite number of states, are presented here.

In the two state case (12), it is assumed there is a ground state with energy ϵ_0 and statistical weight g_0 and an excited state with energy ϵ_1 and statistical weight g_1. If we have a total of n particles, with n_0 particles in the ground state and n_1 particles in the excited state, then

$$n = n_0 + n_1 \ . \qquad \text{(Eq. 25)}$$

Representing the probability per unit time of a particle going from state i to state j by k_{ij}, we have for the time rate of change of n_1,

$$\frac{dn_1}{dt} = k_{01}n_0 - k_{10}n_1 \ . \qquad \text{(Eq. 26)}$$

Using Equation 25, this is

$$\frac{dn_1}{dt} = k_{10}n - (k_{10} + k_{01})n_1 \ . \qquad \text{(Eq. 27)}$$

The solution is

$$n_1 = \frac{k_{01}n}{k_{10} + k_{01}} + n_1^o \exp[-(k_{10} + k_{01})t] \ , \qquad \text{(Eq. 28)}$$

where n_1^o is a constant of integration. This can be written, using Equation 25, as

$$n_1 k_{10} - k_{01} n_0 = n_1^o (k_{10} + k_{01}) \exp[-(k_{10} + k_{01})t] . \qquad \text{(Eq. 29)}$$

At equilibrium, i.e. when $t \to \infty$, we have

$$\frac{\bar{n}_0}{\bar{n}_1} = \frac{k_{10}}{k_{01}} \qquad \text{(Eq. 30)}$$

where the bars over the n_0 and n_1 are used to indicate equilibrium values. The condition for statistical equilibrium is

$$\frac{\bar{n}_0}{\bar{n}_1} = \frac{g_0}{g_1} \exp[-(\epsilon_1 - \epsilon_0)/kT] . \qquad \text{(Eq. 31)}$$

Combining Equations 30 and 31 we have

$$k_{10} = k_{01} \frac{g_0}{g_1} \exp[-(\epsilon_1 - \epsilon_0)/kT] . \qquad \text{(Eq. 32)}$$

Equation 32, together with the relaxation time defined from Equation 29 as $(k_{10} + k_{01})^{-1}$, yields the following expression:

$$\frac{1}{\tau} = k_{10}[1 + \frac{g_0}{g_1} \exp\{-(\epsilon_1 - \epsilon_0)/kT\}] . \qquad \text{(Eq. 33)}$$

The second case, that of the harmonic oscillator, was first treated by Landau and Teller (17). They assume an infinite number of states but that transitions are possible only between adjacent states. The rate of change of particles in the j^{th} state then is given by

$$\frac{dn_j}{dt} = k_{j-1,j}n_{j-1} + k_{j+1,j}n_{j+1} - k_{j,j+1}n_j - k_{j,j-1}n_j \qquad \text{(Eq. 34)}$$

The lowest state, $j = 0$, can only change by transitions with the state $j = 1$, so

$$\frac{dn_0}{dt} = k_{10}n_1 - k_{01}n_0 \cdot \qquad \text{(Eq. 35)}$$

At equilibrium all the $\frac{dn_j}{dt}$ are zero so we can write

$$0 = k_{j-1,j}\bar{n}_{j-1} + k_{j+1,j}\bar{n}_{j+1} - k_{j,j+1}\bar{n}_j - k_{j,j-1}\bar{n}_j \cdot \qquad \text{(Eq. 36)}$$

Starting with

$$0 = k_{10}\bar{n}_1 - k_{01}\bar{n}_0 \qquad \text{(Eq. 37)}$$

and working progressively upward one has

$$0 = k_{j+1,j}\bar{n}_{j+1} - k_{j,j+1}\bar{n}_j \ . \qquad \text{(Eq. 38)}$$

This together with the condition for statistical equilibrium yields

$$\frac{k_{j,j+1}}{k_{j+1,j}} = \frac{\bar{n}_{j+1}}{\bar{n}_j} = \frac{g_{j+1}}{g_j} \exp\left(-\frac{\epsilon_{j+1} - \epsilon_j}{kT}\right) \cdot \qquad \text{(Eq. 39)}$$

Landau and Teller used three properties of transitions in harmonic oscillators in solving the problem. First, all energy differences between adjacent states are the same, namely $h\nu$. Second, all rate constants are proportional to the j of the higher state, i.e.

$$\frac{k_{j+1,j}}{k_{j,j-1}} = \frac{j+1}{j} \ . \qquad \text{(Eq. 40)}$$

Thirdly, all weight factors g_j are unity so that Equation 39 becomes

$$G = \frac{k_{j,j+1}}{k_{j+1,j}} = \exp\left(-\frac{h\nu}{kT}\right) \ , \qquad \text{(Eq. 41)}$$

where G is constant. The rate equations then become

$$\frac{dn_j}{dt} = k_{10}[Gjn_{j-1} + (j+1)n_{j+1} - G(j+1)n_j - jn_j] \qquad \text{(Eq. 42)}$$

and

$$\frac{dn_0}{dt} = k_{10}(n_1 - Gn_0) \quad . \qquad \text{(Eq. 43)}$$

Multiplying Equation 42 by $jh\nu$ and summing over all j from 1 to ∞ we have,

$$h\nu \frac{d}{dt} \sum_{j=1}^{\infty} jn_j = h\nu k_{10} \sum_{j=1}^{\infty} [Gj^2 n_{j-1} + j(j+1)n_{j+1} - Gj(j+1)n_j - j^2 n_j] \quad . \qquad \text{(Eq. 44)}$$

Changing the j to $j - 1$ in the second sum on the right, it now reads

$$\sum_{j=0}^{\infty} j(j-1)n_j \quad . \qquad \text{(Eq. 45)}$$

Combining this with the fourth sum and changing the lower limit of j to zero since the $j = 0$ term contributes nothing, we have

$$\sum_{j=0}^{\infty} [-j^2 + j(j-1)n_j] = -\sum_{j=0}^{\infty} jn_j \quad . \qquad \text{(Eq. 46)}$$

The first and third terms can be combined in the following manner:

$$G \sum_{j=1}^{\infty} j^2 n_{j-1} - G \sum_{j=1}^{\infty} j(j+1)n_j =$$

$$G\left[\sum_{j=0}^{\infty} (j+1)^2 n_j - \sum_{j=0}^{\infty} j(j+1)n_j\right] = G \sum_{j=0}^{\infty} (jn_j + n_j) \ . \qquad \text{(Eq. 47)}$$

The entire sum then reduces to

$$h\nu \frac{d}{dt} \sum_{j=0}^{\infty} jn_j = h\nu k_{10} \sum_{j=0}^{\infty} [(G-1)jn_j + Gn_j] \ . \qquad \text{(Eq. 48)}$$

Since for harmonic oscillators the total energy can be written as

$$E = \sum_{j=0}^{\infty} (j + \tfrac{1}{2})h\nu n_j \qquad \text{(Eq. 49)}$$

we can write

$$\frac{dE}{dt} = -k_{10}(1-G)E + \tfrac{1}{2}k_{10}(1+G)h\nu n \ , \qquad \text{(Eq. 50)}$$

where $n = \sum_{j=0}^{\infty} n_j$.

One can then define the relaxation time as

$$\frac{1}{\tau} = k_{10}(1 - G) = k_{10} - k_{01} \cdot$$

$$= k_{10}[1 - \exp(-h\nu/kT)] \qquad \text{(Eq. 51)}$$

At low temperatures the harmonic oscillator can be treated as a two state system with only the $j = 0$ and $j = 1$ states occupied. In that case Equations 33 and 51 both reduce to $\tau^{-1} \cong k_{10}$. However, this is generally not possible so Equation 51 should be used since the energy states of a polyatomic molecule more closely resemble those of the harmonic oscillator than those of the two state system.

If one defines P_{10} as the probability that a single collision will produce an energy transfer, then

$$k_{10} = \tilde{R}\, P_{10} \,, \qquad \text{(Eq. 52)}$$

where $\tilde{R}$ is the collision rate of the gas molecules. One then has

$$Z_{10} = \frac{1}{P_{10}} = \tilde{R}\, \tau\, [1 - \exp(-h\nu/kT)] \,, \qquad \text{(Eq. 53)}$$

where Z_{10} is the number of collisions required per energy transfer and is called the "collision lifetime." Here one should use τ_m for τ, i.e. the relaxation time of the

exchange mode.

1. Relaxation in mixtures

Consider a mixture of two gases, A and B. Each of these gases is assumed to have a single relaxation time when by itself. Let τ_{AA} be the relaxation time of a single A molecule in a pure A gas and τ_{AB} the relaxation time for an A molecule in an otherwise pure B gas. If X represents the mole fraction of gas A present, we have for the net number of deactivations per unit time of an A molecule due to A - A collisions,

$$k_{10}^{AA} - k_{01}^{AA} = \frac{X}{\tau_{AA}} . \qquad \text{(Eq. 54)}$$

The net number of deactivations per unit time of an A molecule due to A - B collisions is

$$k_{10}^{AB} - k_{01}^{AB} = \frac{(1 - X)}{\tau_{AB}} . \qquad \text{(Eq. 55)}$$

Combining these, we have for the total number of deactivations per unit time of A molecule in the mixture,

$$\frac{1}{\tau_A} = \frac{X}{\tau_{AA}} + \frac{(1 - X)}{\tau_{AB}} . \qquad \text{(Eq. 56)}$$

Similarly an expression for the total number of deactivations per unit time made by a B molecule in the mixture can be found to be

$$\frac{1}{\tau_B} = \frac{(1 - X)}{\tau_{BB}} + \frac{X}{\tau_{BA}} . \qquad \text{(Eq. 57)}$$

If a single relaxation time is observed in the mixture itself, the total number of deactivations per unit time for a molecule in the mixture should be

$$\frac{1}{\tau} = \frac{X}{\tau_A} + \frac{(1 - X)}{\tau_B} . \qquad \text{(Eq. 58)}$$

Combining this with Equations 56 and 57 we have

$$\frac{1}{\tau} = \frac{X^2}{\tau_{AA}} + \frac{(1 - X)^2}{\tau_{BB}} + X(1 - X)\left(\frac{1}{\tau_{AB}} + \frac{1}{\tau_{BA}}\right) , \qquad \text{(Eq. 59)}$$

or a quadratic dependence of τ^{-1} on concentration.

If gas B is non-dispersive, τ_{BB}^{-1} and τ_{BA}^{-1} are zero, so Equation 59 reduces to

$$\frac{1}{\tau} = \frac{X^2}{\tau_{AA}} + X(1 - X)\frac{1}{\tau_{AB}} . \qquad \text{(Eq. 60)}$$

This equation, however, has been shown to be invalid by Olson and Legvold (21) for several halomethane-inert gas mixtures. Their results showed that the observed

relaxation times obey the relation,

$$\frac{1}{\tau} = \frac{X}{\tau_{AA}} + \frac{(1 - X)}{\tau_{AB}} , \qquad \text{(Eq. 61)}$$

rather than 60. The question then is whether Equation 59 is valid for mixtures of two dispersive gases.

This question can be partially resolved by using a somewhat more sophisticated approach in obtaining Equation 59. If one assumes parallel excitation for the A and B molecules, then one can substitute a frequency dependent specific heat of the form,

$$C(\omega) = (C_\infty)_{eff} + \frac{C_A X}{1 + i\omega\tau_A} + \frac{C_B(1 - X)}{1 + i\omega\tau_B} , \qquad \text{(Eq. 62)}$$

into Equation 3. The resulting complex velocity expression is

$$V_\omega^2 = \frac{RT}{M}\left\{1 + \frac{R}{C_\infty \tau_A \tau_B} \frac{(1 + i\omega\tau_A)(1 + i\omega\tau_A)}{(i\omega)^2 + \left[\frac{1}{\tau_A} + \frac{1}{\tau_B} + \frac{C_A X}{C_\infty \tau_A} + \frac{C_B(1-X)}{C_\infty \tau_B}\right] i\omega + \frac{C_o}{C_\infty \tau_A \tau_B}}\right\} . \qquad \text{(Eq. 63)}$$

Here C_A and C_B are the vibrational specific heats of gases A and B, respectively, C_∞ is the effective specific heat of the mixture at high frequencies, and M is the effective molecular weight of the mixture. Throughout the remainder of this discussion the effective notation will be dropped

from all molecular weights and specific heats, and the effective quantities will be implied when mixtures are being discussed. Treating the denominator under $(1 + i\omega\tau_A)(1 + i\omega\tau_B)$ as a quadratic in $(i\omega)$ we find the roots to be $-(\tau')^{-1}$ and $-(\tau'')^{-1}$ and can write Equation 63 as

$$V_\omega^2 = \frac{RT}{M}\left[1 + \frac{R\tau'\tau''}{C_\infty \tau_A\tau_B}\frac{(1 + i\omega\tau_A)(1 + i\omega\tau_B)}{(1 + i\omega\tau')(1 + i\omega\tau'')}\right] . \qquad \text{(Eq. 64)}$$

The fraction involving the $(i\omega\tau)$'s can now be written, using the method of partial fractions, as

$$\frac{\tau_A\tau_B}{\tau'\tau''} + \frac{A'}{1 + i\omega\tau'} + \frac{B'}{1 + i\omega\tau''} \qquad \text{(Eq. 65)}$$

where

$$A' = \frac{1}{\tau'}(\tau' - \tau_A)(\tau' - \tau_B)(\tau' - \tau'')^{-1}$$

and

$$B' = \frac{1}{\tau''}(\tau'' - \tau_A)(\tau'' - \tau_B)(\tau'' - \tau')^{-1} .$$

V^2 then becomes

$$V^2 = \frac{RT}{M}\left\{1 + \frac{R}{C_\infty}\left[1 + \frac{A''}{1 + i\omega\tau'} + \frac{B''}{1 + i\omega\tau''}\right]\right\} , \qquad \text{(Eq. 66)}$$

where

$$A'' = \frac{\tau'\tau''}{\tau_A\tau_B} A'$$

and

$$B'' = \frac{\tau'\tau''}{\tau_A\tau_B} B' \ .$$

It has been indicated (20) that the times, τ' and τ'', can be interpreted as the observed relaxation times of the mixture. Assuming this to be true, we have for the values of τ' and τ'', from the roots of $(i\omega)$ in Equation 63,

$$\frac{1}{\tau'}, \frac{1}{\tau''} = \frac{1}{2}\left[\frac{1}{\tau_A} + \frac{1}{\tau_B} + \frac{C_A}{C_\infty}\frac{X}{\tau_A} + \frac{C_B}{C_\infty}\frac{(1 - X)}{\tau_B}\right]$$

$$\pm \frac{1}{2}\left\{\left[\frac{1}{\tau_A} + \frac{1}{\tau_B} + \frac{C_A}{C_\infty}\frac{X}{\tau_A} + \frac{C_B}{C_\infty}\frac{(1 - X)}{\tau_B}\right]^2 - \frac{4C_o}{C_\infty}\frac{1}{\tau_A\tau_B}\right\}^{\frac{1}{2}} . \qquad \text{(Eq. 67)}$$

For the case where gas B is non-dispersive, i.e. where τ_B^{-1} is zero, Equation 67 reduces to

$$\frac{1}{\tau'}, \frac{1}{\tau''} = \frac{1}{\tau_A} + \frac{C_A}{C_\infty}\frac{X}{\tau_A}, \ 0$$

$$= \frac{C_o}{C_\infty}\frac{1}{\tau_A}, \ 0 \ . \qquad \text{(Eq. 68)}$$

When the previously defined expression for τ_A^{-1} is inserted into the first solution, the desired linear relation is obtained.

Calvert and Amme (5) have shown that, for the case where $C_A \cong C_B$ and $\tau_A \cong \tau_B$, Equation 67 reduces to

$$\frac{1}{\tau'}, \frac{1}{\tau''} = \frac{C_o}{C_\infty}\left(\frac{X}{\tau_A} + \frac{1 - X}{\tau_B}\right), \frac{1 - X}{\tau_A} + \frac{X}{\tau_B} . \qquad \text{(Eq. 69)}$$

The vibrational specific heat associated with the first solution is almost the full value for the mixture and that associated with the second is almost zero. Therefore, the observed results will appear as though there were a single relaxation time. When τ_A^{-1} and τ_B^{-1} are inserted into Equation 69, the quadratic dependence on concentration is obtained.

F. Energy Exchange Theory

1. Landau and Teller results

Several theories predicting the efficiency of molecular collisions in transferring energy from one degree of freedom to another have been worked out. In general, these theories are based on the assumption that binary collisions are predominately responsible for energy transfers. This

assumption has been experimentally verified (12) by showing that the rate of energy exchange is proportional to the pressure, thus enabling one to plot the experimental results of the dispersion phenomena against f/P rather than against f. That is, doubling the sonic frequency has the same effect as halving the pressure.

As has been stated earlier, the first important contribution to the energy exchange theory was made by Landau and Teller (17). They took into account Maxwell's distribution law for relative velocities and pointed out the importance of Ehrenfest's adiabatic principle in energy transfer problems.

Adiabatic and non-adiabatic processes as pertaining to periodic motion are defined as follows: If one changes a parameter (e.g. the strength of an external field) and the relative change of this parameter is small during a period of the motion the process is said to be (nearly) adiabatic. It is non-adiabatic if the relative change is large. Ehrenfest has shown that an adiabatic change in a quantum system does not alter the state of the system; i.e. the same quantum numbers used to describe the system before the change are also valid after the change, although there may be a change of phase. This is not true for a non-adiabatic change.

A classical analogue is presented by Landau and

Teller. Consider a diatomic (b-c) molecule with the (c) atom fixed in space (as though it had infinite mass). An (a) molecule approaches in the (b-c) direction and strikes the (b) atom. If (a) and (b) are hard spheres and $m_a < m_b$, (a) will rebound and (b) will be knocked towards (c), compressing the "spring" between them. Here m_a and m_b are the masses of the (a) molecule and the (b) atom, respectively. (b)'s motion will eventually change direction and it will move back to the point where it was initially struck. Since (a) is no longer there, (b) will continue on and harmonic motion will result. This is an extreme example of a non-adiabatic process since the (b-c) molecule now has internal energy and the (a) molecule has less energy than before the collision.

An adiabatic change would result if a long range repulsive potential existed between (a) and (b). In this case the (b) atom would begin to move towards (c) long before (a) reached (b) and (a) would begin to slow down. At some point (a) and (b) will both stop and the process will be reversed. (b) will ultimately reach its original position and stop and (a) will have all its kinetic energy back. The result is that no energy has been transferred from (a) to (b-c) and the process is adiabatic.

From this analogy Landau and Teller concluded that the probability of energy transfer is dependent on and

increases with the ratio of the period of vibration of (b-c) to the time of interaction with (a). If one calls the range of interaction s and the relative velocities of the two molecules w, then the time of interaction is s/w. The probability of energy transfer should then increase as a function of $(w/\nu s)$, where ν is the frequency of vibration. Since the range of the attractive forces are large compared with the range of the repulsive forces, Landau and Teller concluded that only the latter need be considered. The attractive forces, however, are influential in that they tend to increase the relative velocities of the molecule prior to the collision.

Using an exponential interaction potential they found that the probability for an energy transfer was of the form

$$P_{10} = \frac{1}{Z_{10}} = \frac{1}{Z_o} \exp(-2\pi\nu s/w) \qquad \text{(Eq. 70)}$$

where Z_o is a pure number of order unity. This must then be averaged over Maxwell's distribution for relative velocities. This yields the following expression for Z_{10}:

$$\frac{1}{Z_{10}} = \frac{1}{Z_o} \frac{\mu}{kT} \int_{-\infty}^{\infty} wdw \exp\left(-\frac{2\pi\nu s}{w} - \frac{\mu w^2}{2kT}\right) , \qquad \text{(Eq. 71)}$$

where μ is the reduced mass of the colliding molecules,

i.e.

$$\mu = \frac{m_a(m_b + m_c)}{m_a + m_b + m_c} \quad . \qquad \text{(Eq. 72)}$$

The integral was approximately evaluated using the fact that the main contribution to the integral comes when the exponent is a minimum. This condition is obtained when the relative velocity is given by

$$w_m = \left(\frac{2\pi\nu skT}{\mu}\right)^{1/3} \quad . \qquad \text{(Eq. 73)}$$

This is the relative velocity that will most probably cause an energy transfer and will be useful later on. The final result of Landau and Teller's work is

$$\frac{1}{Z_{10}} = \frac{1}{Z_o}\sqrt{\frac{2\pi}{3}}\left(\frac{\epsilon'}{kT}\right)^{1/6}\exp\left[-\frac{3}{2}\left(\frac{\epsilon'}{kT}\right)^{1/3}\right] , \qquad \text{(Eq. 74)}$$

where

$$\epsilon' = \mu(2\pi\nu s)^2 \quad .$$

2. Quantum mechanical treatment

The quantum mechanical treatment of this problem is discussed by Herzfeld and Litovitz (12) and the work of several people is presented. In general a one dimensional picture is first considered and the results are then

generalized to three dimensions.

The first theory presented is that due to Jackson and Mott (14). The actual application of Jackson and Mott's work to this problem was made by Schwartz et al. (31). They considered a diatomic molecule (b-c) fixed in space with a parallel stream of (a) molecules approaching along the (b-c) axis with a velocity equal to the relative velocity of the two molecules. The (b-c) molecule is assumed to have two energy levels, E_o and E_1, corresponding to the ground state and the first excited state respectively. An (a) molecule can then be scattered either elastically with $E_a^{(2)} = E_a^{(1)}$, or inelastically with $E_a^{(2)} = E_a^{(1)} \pm h\nu$, where $E_a^{(1)}$ and $E_a^{(2)}$ are the kinetic energies of the (a) molecule before and after the collision, respectively, and $h\nu = E_1 - E_o$. The ratio of the number of particles scattered in unit time with $E_a^{(2)} = E_a^{(1)} - h\nu$ to the total number scattered in unit time is the probability that an excitation will occur during a collision. Its reciprocal is the number of collisions required per excitation. Similarly, the ratio of the number of molecules scattered in unit time with $E_a^{(2)} = E_a^{(1)} + h\nu$ to the total number scattered is the reciprocal of the number of collisions required per de-excitation.

In treating the one dimensional problem, Jackson and Mott used the potential

$$\varphi_1 = \varphi_o \exp(-x/s) \ , \qquad \text{(Eq. 75)}$$

where x is the distance between the (a) molecule and the center of mass of the (b-c) molecule. Their result is

$$k_{10} = \frac{1}{Z_o} \frac{1}{Z_{osc}} \frac{1}{Z_{tr}} \ , \qquad \text{(Eq. 76)}$$

where

$$Z_{osc} = \frac{1}{\pi^2} \frac{\theta'}{\theta} \frac{m_b m_c}{m_b^2 + m_c^2} \frac{m_a + m_b + m_c}{m_a} \ ,$$

$$Z_{tr} = \pi^2 \sqrt{\frac{3}{2\pi}} \left(\frac{\theta}{\theta'}\right)^2 \left(\frac{T}{\theta'}\right)^{1/6} \exp\left[\frac{3}{2}\left(\frac{\theta'}{T}\right)^{1/3} - \frac{\theta}{2T}\right] \ ,$$

$$\theta = \frac{h\nu}{k} \ , \qquad \text{and} \qquad \theta' = \frac{16\pi^2 \mu s^2 \nu^2}{k} \ .$$

Using Equation 53 we have

$$Z_{10} = Z_o Z_{osc} Z_{tr} [1 - \exp(-\theta/T)]^{-1} \ . \qquad \text{(Eq. 77)}$$

$\tilde{R}$ does not appear in this equation since in the above work the flow of incident particles was normalized to one per second.

The exponential interaction potential used by Jackson and Mott was chosen to some extent for its mathematical convenience and in reality is not correct since it contains

no attractive part. The Lennard-Jones interaction potential,

$$\varphi_2 = 4\epsilon[(\frac{r_o}{r})^{12} - (\frac{r_o}{r})^6] , \qquad \text{(Eq. 78)}$$

has been used quite successfully in theoretical calculations of various properties of many gases. This potential has also been applied to the energy exchange problem by fitting it at small r to the exponential of the type used by Jackson and Mott. Since Equation 78 has a minimum of $-\epsilon$, the potential

$$\varphi_1' = \varphi_o e^{-r/s} - \epsilon \qquad \text{(Eq. 79)}$$

was used instead of Equation 75.

Schwartz et al. (31) fitted Equation 78 to Equation 79 by making the two curves tangent at the classical turning point, r_c, of the (a) molecule. de Wette and Slawsky (6) fitted the curves by making them equal at two points, r_c and r_o. r_o is defined by $\varphi_2(r_o) = 0$. The results of the two methods do not differ by much. Schwartz et al. found that the ratio r_o/s should be about 17.5 and de Wette and Slawsky found this ratio to be about 18.6. The use of Equation 79 in Jackson's and Mott's work leads to an additional factor of $\exp(-\epsilon/kT)$ in the expression for Z_{10}.

This factor, together with a value of s obtained from the ratio r_o/s, allow one to find realistic values for Z_{10}.

The three dimensional problem is solved by Schwartz and Herzfeld (30) assuming that the (b-c) molecule is spherically symmetric and that the vibrations correspond to a symmetric increase and decrease of the size of the sphere. This assumption permits the problem to be treated neglecting the rotation of the molecule and results in cylindrical symmetry about the incident direction of the (a) molecules. The three dimensional problem then reduces essentially to the one dimensional problem with the addition of a quasi potential due to centrifugal acceleration. Schwartz and Herzfeld consider this quasi potential to have the greatest effect at the point $r = r_c$ and replace it by a constant term evaluated at that point. They also consider the effect of the increased velocity due to the attractive potential and obtain the following expression:

$$Z_{10} = 1.017\left(\frac{r_o}{r_c}\right)^2 Z_o Z_{osc} Z_{tr} Y \exp(-\epsilon/kT)[1 - \exp(-\theta/T)]^{-1} . \qquad \text{(Eq. 80)}$$

Here Y is a monotonously decreasing function of kT/ϵ and can be calculated to within 2% for $0.70 \leq kT/\epsilon \leq 10$ from the expression

$$Y = 0.76\ (1 + 1.1\ \epsilon/kT) . \qquad \text{(Eq. 81)}$$

Amme and Legvold (2) applied the above theory to several substituted methane molecules and found that for better agreement a shorter repulsive range was required. Hamann and Lambert (10) proposed that for quasi-spherical molecules, such as the methane derivatives, one should use a steeper repulsive potential. In the spirit of the Schwartz et al. method, Amme and Legvold (3) fitted a Lennard-Jones type potential with a steeper repulsive part to the exponential potential. The potential function used was

$$\varphi_2' = 4\epsilon[(\frac{r_o}{r})^{28} - (\frac{r_o}{r})^7] \ . \qquad \text{(Eq. 82)}$$

They found the ratio r_o/s to be about 34. Applying this innovation to mixtures of $CHClF_2$ with argon and helium, they found the predicted values of Z_{10}^{AB} to agree quite well with those found experimentally. Here Z_{10}^{AB} is the number of collisions an A molecule must make with B molecules per deexcitation. Further credence in this method is found in the work of Olson and Legvold (21). They applied this method to several mixtures of halomethane gases with noble gases and found the results quite good.

In this work the potential,

$$\varphi_2'' = \frac{4}{3}^{4/3} \epsilon[(\frac{r_o}{r})^{28} - (\frac{r_o}{r})^7] \ , \qquad \text{(Eq. 83)}$$

was used rather than Equation 82. Equation 83 has a minimum value of $-\epsilon$ and is more comparable with Equation 79 than is Equation 82. This function was then made tangent to Equation 79 at the point r_c by equating both the functions and their derivatives at that point. This resulted in the relations,

$$\frac{r_o}{s} = \frac{7(4)^{4/3}}{3} \left(\frac{r_o}{r_c}\right) \left[4\left(\frac{r_o}{r_c}\right)^{28} - \left(\frac{r_o}{r_c}\right)^{7}\right] \frac{1}{1 + E_m/\epsilon} \qquad \text{(Eq. 84)}$$

and

$$\frac{E_m}{\epsilon} = \frac{4^{4/3}}{3} \left[\left(\frac{r_o}{r_c}\right)^{28} - \left(\frac{r_o}{r_c}\right)^{7}\right] . \qquad \text{(Eq. 85)}$$

E_m here is the most effective energy of collision and is given by

$$E_m = \tfrac{1}{2}\mu w_m^2 . \qquad \text{(Eq. 86)}$$

w_m is the relative velocity that will most probably cause an energy transfer and can be obtained from Equation 73. A plot of r_o/s vs. E_m/ϵ is shown in Figure 1.

3. Application to mixtures

Since τ_{AB}^{-1} and τ_{BA}^{-1} appear in Equation 59 as a sum, it is impossible to find experimental values for these

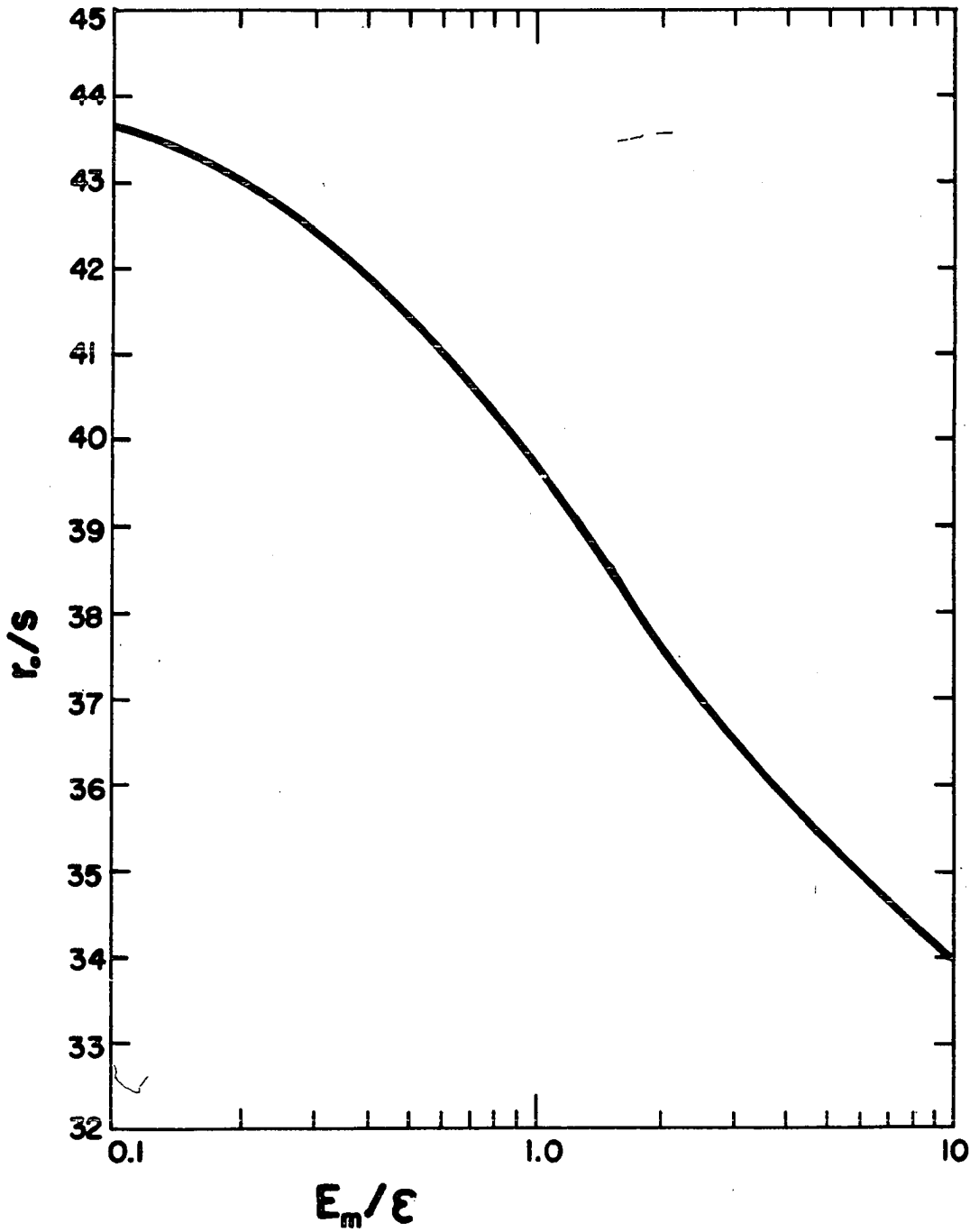

Fig. 1 r_o/s vs. E_m/ε for $\Phi = \frac{4^{4/3}\varepsilon}{3}\left[\left(\frac{r_o}{r}\right)^{28} - \left(\frac{r_o}{r}\right)^{7}\right]$

quantities separately. Hence, one cannot use Equation 53 to find experimental values for Z_{10}^{AB} and Z_{10}^{BA}. One can, however, combine Equations 53 and 80 and find theoretical values for τ_{AB}^{-1} and τ_{BA}^{-1} individually and compare their sum with the value of $(\tau_{AB}^{-1} + \tau_{BA}^{-1})$ found experimentally.

In the following discussion all quantities labeled AB refer to interactions in which a B molecule is impinging upon an A molecule. Quantities labeled BA refer to interactions with an A molecule impinging upon a B molecule. Those labeled AA or A and BB or B refer to interactions involving like molecules. A relation for τ_{AB}^{-1} will be derived and one for τ_{BA}^{-1} can be deduced by interchanging the roles of A and B in the labeling.

If we divide Z_{10}^{AB}, obtained from Equation 80, by Z_{10}^{AA}, obtained from the same equation, and assume $Z_o^{AB} = Z_o^{AA}$ we have

$$\frac{Z_{10}^{AB}}{Z_{10}^{AA}} = \left(\frac{r_o^{AB}}{r_c^{AB}}\right)^2 \left(\frac{r_c^{A}}{r_o^{A}}\right)^2 \frac{Z_{osc}^{AB}}{Z_{osc}^{A}} \frac{Z_{tr}^{AB}}{Z_{tr}^{A}} \frac{Y_{AB}}{Y_A}$$

$$X \exp[-(\epsilon_{AB} - \epsilon_A)/kT] \frac{1 - \exp(-\theta_A/T)}{1 - \exp(-\theta_{AB}/T)} . \qquad \text{(Eq. 87)}$$

Further, assuming that $(r_o^{AB}/r_c^{AB}) \cong (r_o^{A}/r_c^{A})$ and that the

fraction $\frac{m_b m_c}{m_b^2 + m_c^2}$ in Z_{osc} will be the same for the AA term as for the AB term, since in both cases the (b-c) molecule is the A molecule, we have

$$\frac{Z_{10}^{AB}}{Z_{10}^{AA}} = \frac{M_A + M_B}{2M_B} \frac{\theta_{AB}}{\theta_A} \left(\frac{\theta'_A}{\theta'_{AB}}\right)^{7/6} \frac{Y_{AB}}{Y_A} \frac{1 - \exp(-\theta_A/T)}{1 - \exp(-\theta_{AB}/T)}$$

$$X \exp\left[\frac{3}{2}\left(\frac{\theta'_{AB}}{T}\right)^{1/3} - \frac{3}{2}\left(\frac{\theta_A}{T}\right)^{1/3} + \frac{\theta_A - \theta_{AB}}{2T} + \frac{\epsilon_A - \epsilon_{AB}}{kT}\right] . \qquad \text{(Eq. 88)}$$

The molecular weight, M, is now used instead of the mass of the molecules, m, since they differ only by a constant factor and this factor cancels out in the fraction. Now, using Equation 53 to obtain an expression for Z_{10}^{AB}/Z_{10}^{AA}, we have

$$\frac{Z_{10}^{AB}}{Z_{10}^{AA}} = \frac{\tilde{R}_{AB}}{\tilde{R}_A} \frac{\tau_m^{AB}}{\tau_m^{AA}} \frac{1 - \exp(-\theta_{AB}/T)}{1 - \exp(-\theta_A/T)} . \qquad \text{(Eq. 89)}$$

We can now equate Equations 88 and 89 and obtain the following expression for τ_m^{AB}:

$$\frac{1}{\tau_m^{AB}} = \frac{1}{\tau_m^{AA}} \frac{2M_B}{M_A + M_B} \frac{\theta_A}{\theta_{AB}} \left(\frac{\theta'_{AB}}{\theta'_A}\right)^{7/6} \frac{Y_A}{Y_{AB}} \frac{\tilde{R}_{AB}}{\tilde{R}_A} \left[\frac{1 - \exp(-\theta_{AB}/T)}{1 - \exp(-\theta_A/T)}\right]^2$$

$$X \exp\left[\frac{3}{2}\left(\frac{\theta'_A}{T}\right)^{1/3} - \frac{3}{2}\left(\frac{\theta'_{AB}}{T}\right)^{1/3} + \frac{\theta_{AB} - \theta_A}{2T} + \frac{\epsilon_{AB} - \epsilon_A}{kT}\right] .$$

(Eq. 90)

This equation can be further simplified due to the assumption of parallel excitation for the A and B molecules. This assumption means that the exchange mode for the AA terms is the same as for the AB terms or that $\theta_A = \theta_{AB}$. If parallel excitation had not been assumed the exchange mode for A-B collisions would be the exchange mode of either the A molecule or the B molecule, whichever is lower. The condition of parallel excitation also indicates that

$$\tau_m^{AB} = \frac{C_m^A}{C_A} \tau_{AB} \qquad \text{(Eq. 91)}$$

and

$$\tau_m^{AA} = \frac{C_m^A}{C_A} \tau_{AA} \qquad \text{(Eq. 92)}$$

so Equation 90 leads to

$$\frac{1}{\tau_{AB}} = \frac{1}{\tau_{AA}} \frac{2M_B}{M_A + M_B} \left(\frac{\theta'_{AB}}{\theta'_A}\right)^{7/6} \frac{Y_A}{Y_{AB}} \frac{\tilde{R}_{AB}}{\tilde{R}_A}$$

$$X \exp\left[\frac{2}{3}\left(\frac{\theta'_A}{T}\right)^{1/3} - \frac{3}{2}\left(\frac{\theta'_{AB}}{T}\right)^{1/3} + \frac{\epsilon_{AB} - \epsilon_A}{kT}\right] .$$

(Eq. 93)

III. EXPERIMENT

A variable-path acoustic interferometer was used to determine the sound velocity in the gases investigated in this study. Figure 2 is a cross-sectional view of the interferometer. Basically it consists of a movable reflector (labeled F in the figure), whose bottom surface is kept parallel to the upper surface of an X-cut piezoelectric quartz crystal (G). The quartz crystal serves as a source for the sound wave. By moving the reflector up or down, one can determine positions of resonance, i.e. positions where standing waves exist between the crystal and reflector. Since these positions are spaced a distance of $\lambda/2$ apart, where λ is the wave length of the sound wave, the velocity of the sound can be determined from the relation

$$V = f\lambda \ . \qquad \text{(Eq. 94)}$$

The quartz crystal is a squat cylinder in shape, whose surfaces are optically flat and gold plated. It is mounted on three equally spaced, spring loaded prongs (J) which fit into dimples in the nodal plane of the crystal. Electrical contact is made to the upper and lower gold surfaces of the crystal by means of layers of silver paint from two of the mounting prongs.

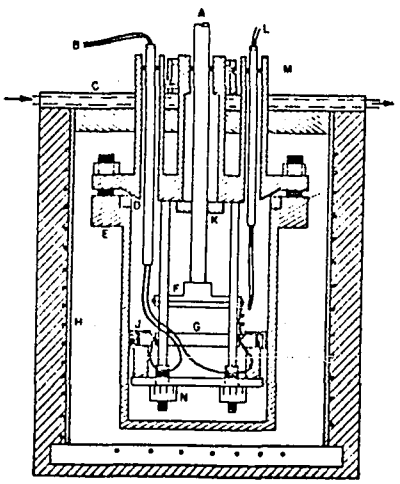

Fig. 2. The interferometer.

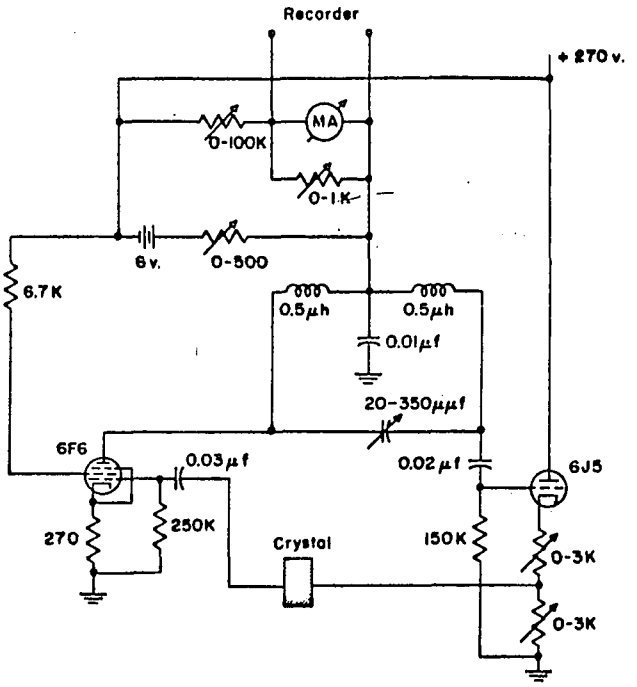

Fig. 3. The crystal oscillator circuit.

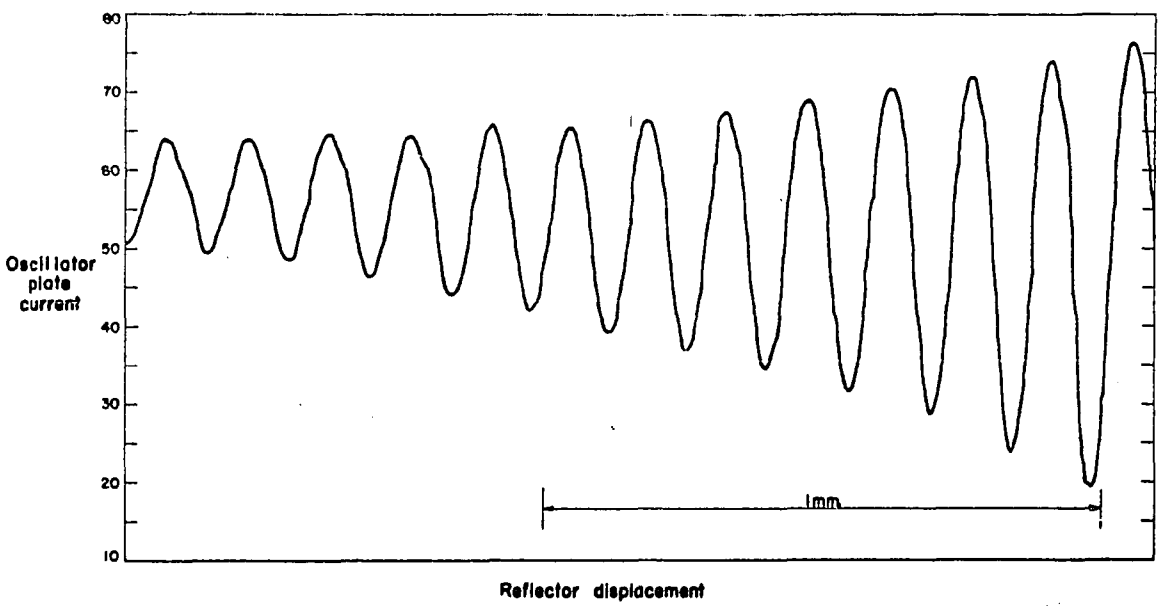

Fig. 4. Oscillator plate current vs. reflector displacement.

The surface of the reflector is also optically flat and gold plated. In order to prevent spurious capacity effects, the upper surface of the crystal and the reflector surface are kept at the same potential by means of a gold connector wire. Parallelism between the surfaces of the crystal and reflector can be obtained by means of three doubly threaded nuts (N).

A micrometer screw is used to move the reflector. It is connected via a machined Invar steel rod (A) to the reflector. The micrometer is a precision instrument manufactured by Gaertner and Company. Its traveling length is 100 mm and it has a least count of 0.001 mm. A precision bushing (K) is used to keep the reflector and crystal parallel while the reflector is being moved.

The entire arrangement is enclosed in a stainless steel cup (E) which is sealed at the top by a Teflon gasket (D). Electrical connections inside the chamber are made through glass tubes which are vaccum sealed with neoprene O-rings at the top. An iron-constantan thermocouple (L) is used in conjunction with a Rubion Co. potentiometer and a Leeds and Northrup galvanometer to determine the temperature of the gas. A thermal jacket (H) surrounds the chamber to keep temperature variations at a minimum.

An opening (not shown in the figure), similar to the

ones through which the glass tubes go, is used to handle the gas. An appropriate valve system permits the chamber to be evacuated and also provides for the filling of the chamber with the gas desired. A fore pump is used to evacuate the chamber and a McLeod gauge is used to measure the vacuum. A mercury monometer is used to measure the pressure of the gas.

The quartz crystal is driven at its fundamental frewuency by an electronic oscillator which is shown schematically in Figure 3. The oscillator is essentially tne same as the one described by Rossing (28). Slight changes have been made to increase sensitivity and reduce noise. The resonance positions of the reflector are determined by a sharp change in the plate current of the oscillator. These can be detected either on the microammeter (labeled MA in the circuit diagram) or on the scale of a Brown chart recorder, which is introduced into the circuit as indicated. A sychronous motor can be used to move the reflector away from the crystal at a constant rate. In that case, a plot of plate current vs. reflector displacement is obtained from the chart recorder. A sample of this plot is shown in Figure 4. The peaks correspond to resonance positions and the troughs to anti-resonance positions. The apparent flutter in the curves is due to a nervous draftsman rather than to noise in the electronics. A 250 ma. electronically

regulated power supply, fed with 115 volts from a 2.5 K.V.A. Stabaline voltage regulator supplies the power for the oscillator. The frequency is measured with a BC-221 frequency meter.

In order to minimize any undesirable effects due to impurities which may cling to the walls of the chamber, the system was evacuated and allowed to outgas for about a day before each run. The pressure maintained throughout the outgasing period was approximately one micron of mercury. Impurity effects can be quite detrimental, especially if these impurities differ greatly in molecular weight from the gas being studied. The gases examined in this study were provided by the E. I. du Pont de Nemours and Company, Freon Products Laboratory. The purities of these gases as quoted by the suppliers are listed in Table 2. Also listed in this table are the molecular weights of the gases, their vibrational specific heats, and the specific heat associates with the exchange mode.

When the system was sufficiently outgassed, the gases to be studied were fed into the system. The method followed in preparing a mixture was the following. One of the gases was first put into the system to a predetermined pressure. The second gas was then fed in to the desired total pressure, usually about one atmosphere. The second gas was fed in at a rather rapid rate to minimize any

Table 2. Values of purity, M, C_{vib}, and C_m at 298°K

Gas	% Purity	M (gm/mole)	C_{vib} (cal/mole-deg)	C_m (cal/mole-deg)
CH_2F_2	99.5	52.03	2.264	1.178
CHF_3	99.9	70.02	4.691	2.462
CF_4	99.9+	88.01	6.669	2.776
CCl_2F_2	99.99+	120.92	8.526	1.745
$CHCl_2F$	99.5	102.93	6.697	1.719

diffusion of the first gas out of the system. The percentage of each gas present was then determined from the laws of partial pressure. In order to obtain a uniform distribution of each gas throughout the chamber, the mixture was allowed to stand for a period of about twelve hours before any velocity measurements were made.

Velocity measurements for this study were made manually rather than with the use of the chart recorder and the synchronous drive. The meter on the chart recorder was, however, used. The manual method is as follows: The micrometer screw was turned until the meter was almost at a peak position. The micrometer setting, as well as the meter reading at this position were recorded. The micrometer screw was then turned until the meter reading

reached the same point on the other side of the peak, where the micrometer setting was again recorded. The mean value of the two micrometer settings was then taken to be a resonance position of the crystal-reflector separation. The reflector was then moved through a known number of peaks and the process was repeated. The difference between the two resonance positions is an integral number of half wavelengths, thus providing a numerical value for the wave length. For the processes described above, the reflector was always moved away from the crystal.

Upon completion of a velocity determination at a given pressure, some of the gas was pumped out and a velocity measurement was made at the new pressure. The pressure, of course, was recorded for each velocity measurement.

Temperature measurements were made at the beginning and the end of each velocity measurement and the average of these was taken for the temperature of the measurement. Throughout a run the temperature variations were small, i.e. less than one degree Centigrade. All velocity measurements were corrected to a uniform temperature by assuming the predominant temperature dependence in V^2 is the linear one occurring in Equation 3. That is, the dependence of C on temperature was neglected.

The frequency was checked periodically during a run to insure that it was remaining constant.

Ideal corrections were then made, and the resulting velocities were squared and plotted against $\log_{10}(f/p)$. This curve was then fitted to one calculated from Equation 9 and an experimental relaxation time was determined.

IV. RESULTS AND DISCUSSION

A. Experiment

The velocity dispersion results for CH_2F_2, CHF_3, CF_4, CCl_2F_2, and $CHCl_2F$ and for mixtures of these gases are graphically presented in Figures 5 through 40. The first five of these figures show velocity dispersion in the pure gases. The remaining figures show velocity dispersion in the mixtures. The dots on all these figures represent the ideally corrected experimental data and the solid curves represent the theoretical velocity calculated from Equation 17. The short vertical lines, labeled f_i = XXX, designate the inflection frequencies of the theoretical curve. These values correspond to experimental inflection frequencies which are normalized to one atmosphere pressure.

With two exceptions, the velocity data fit the theoretical dispersion curves very well. The exceptions are the CHF_3-$CHCl_2F$ mixtures (Figures 29 through 31) and the CF_4-$CHCl_2F$ mixtures (Figures 35 through 37). Several runs of each of these mixtures were made to check the reproducibility of the data. In all cases the data were reproducible to within the limits of experimental error.

In general the points corresponding to data taken at high pressures fit the theoretical curves fairly well.

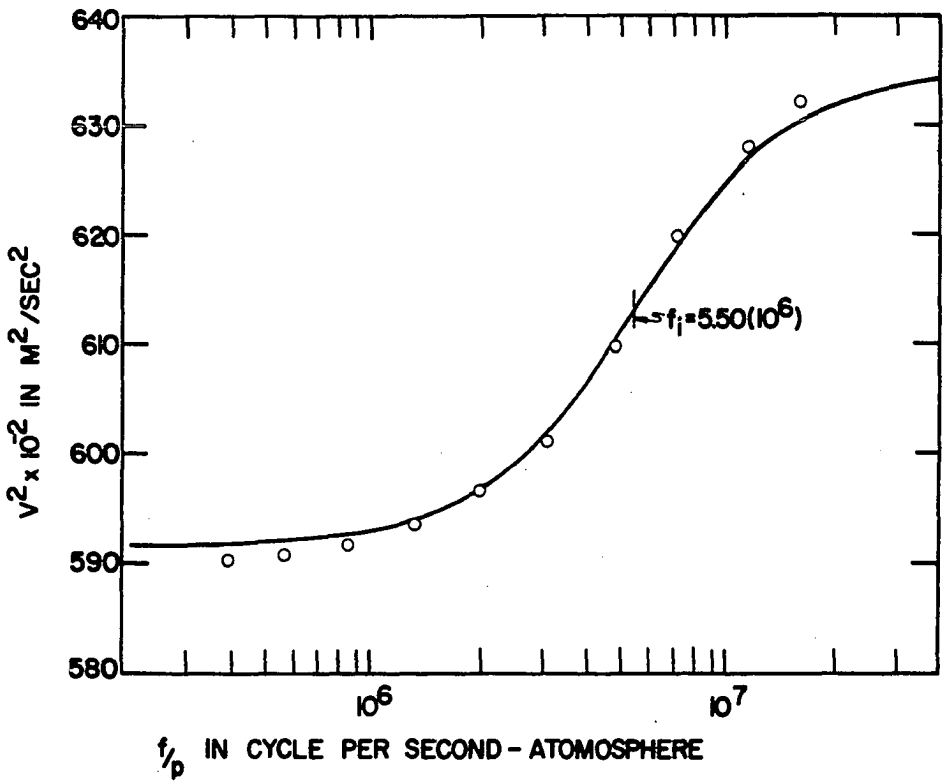

Fig. 5 Velocity dispersion in CH_2F_2 at 298.0° K.

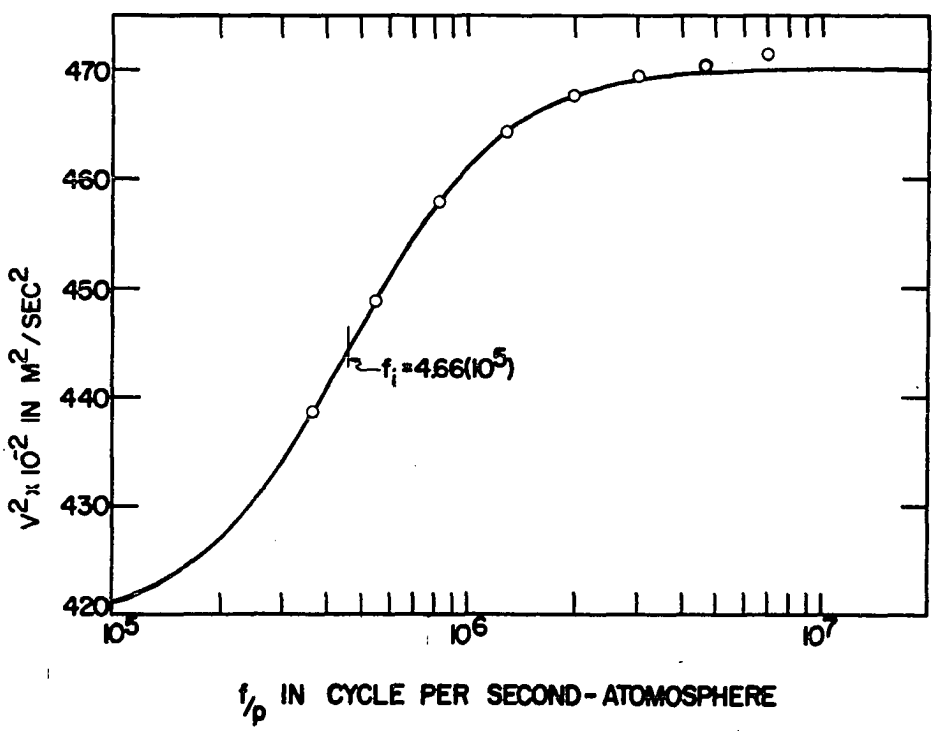

Fig. 6 Velocity dispersion in CHF_3 at 296.9° K.

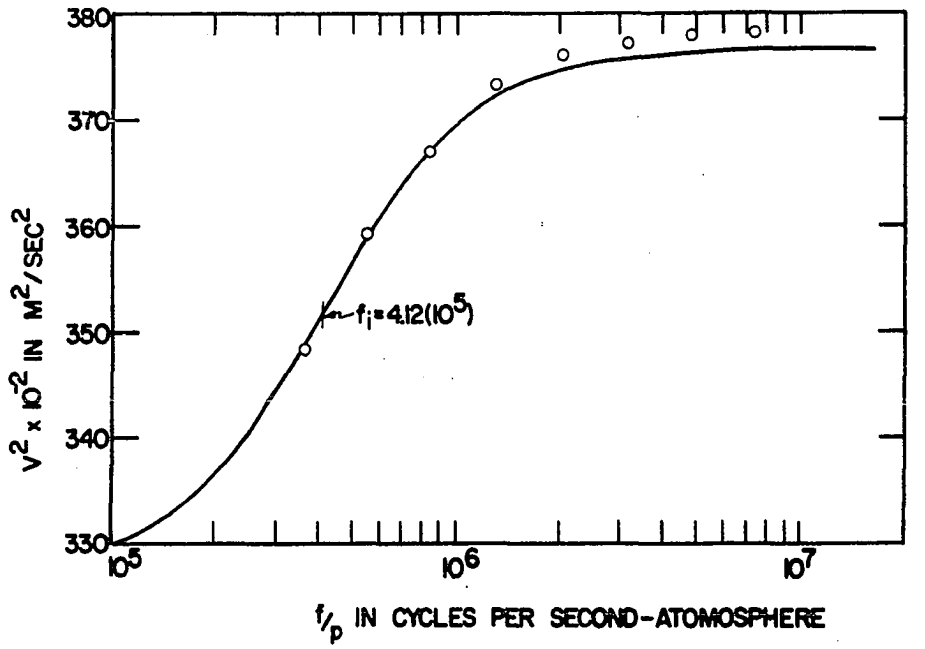

Fig. 7 Velocity dispersion in CF_4 at 298.9° K.

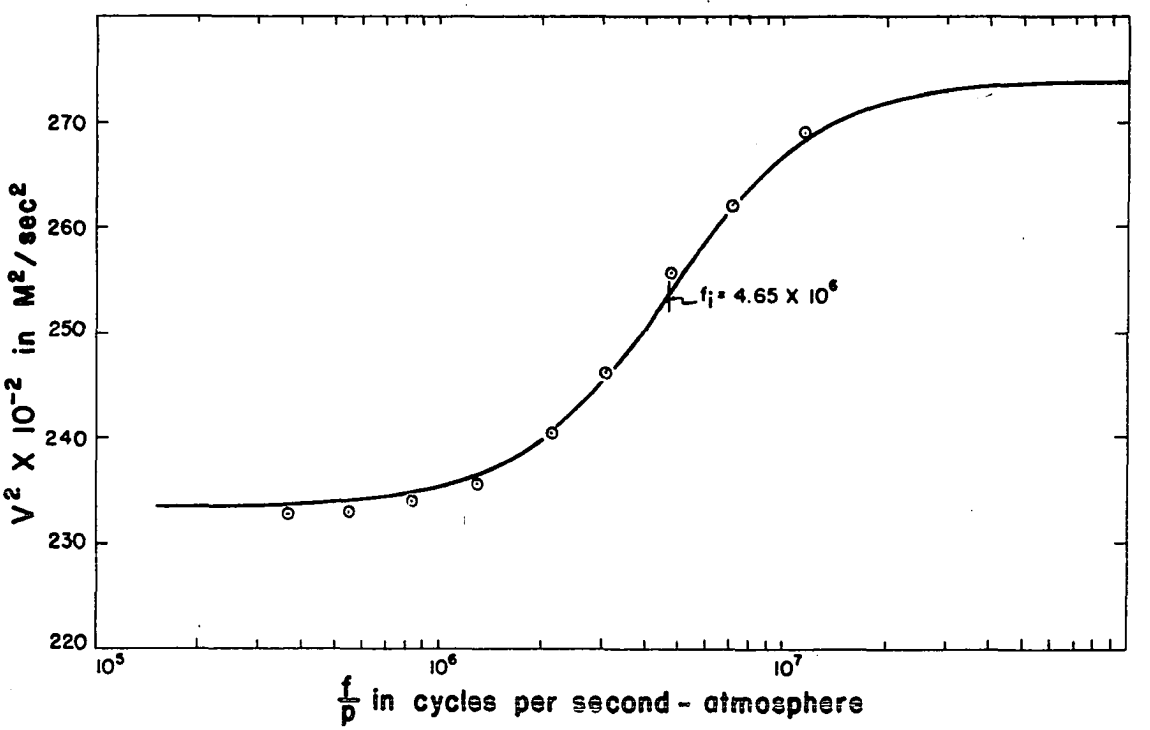

Fig. 8 Velocity dispersion in CCl_2F_2 at 298.4° K.

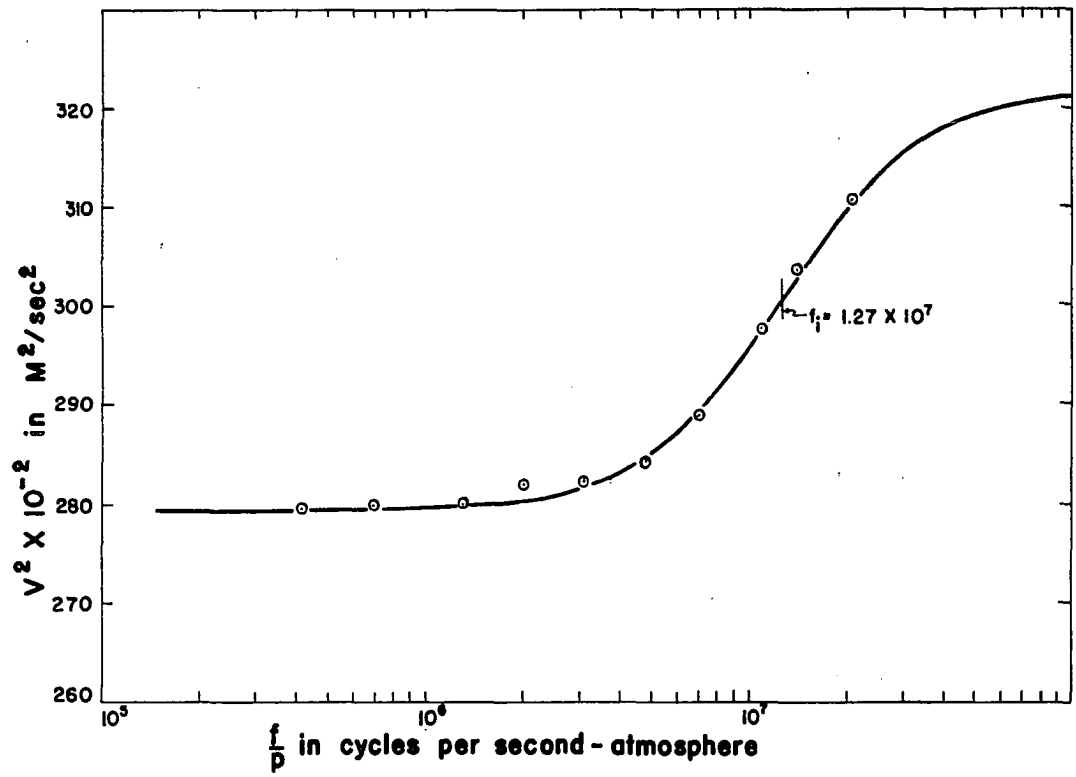

Fig. 9 Velocity dispersion in $CHCl_2F$ at 298.8° K.

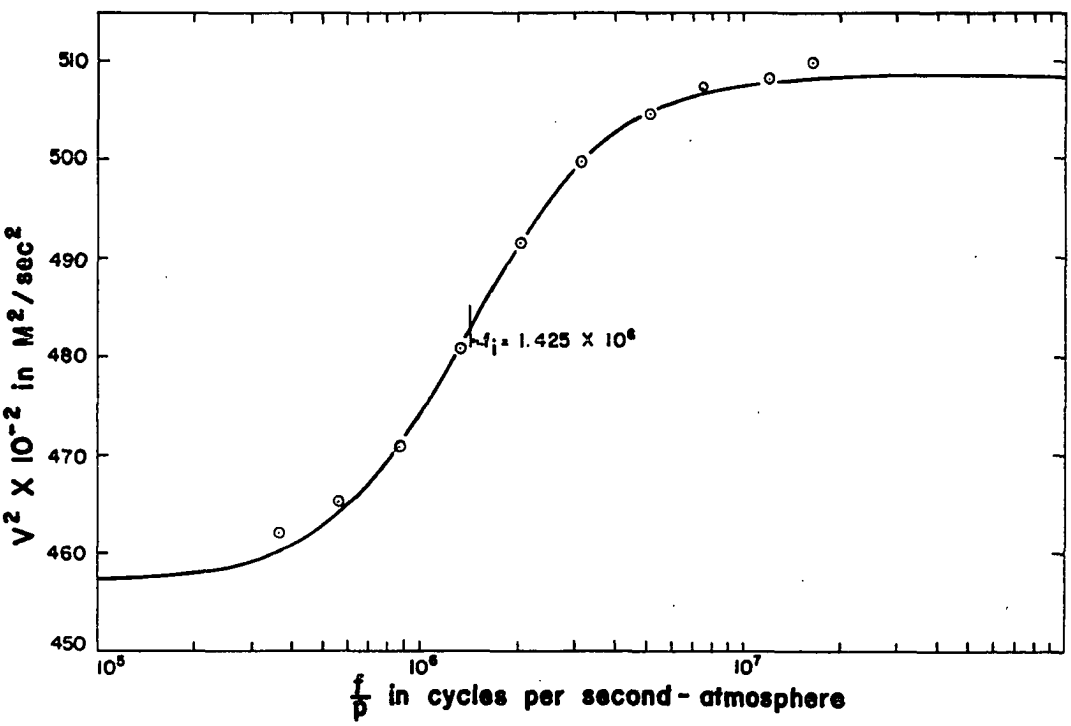

Fig. 10 Velocity dispersion in 26.7% CH_2F_2 - 73.3% CHF_3 at 299.2° K.

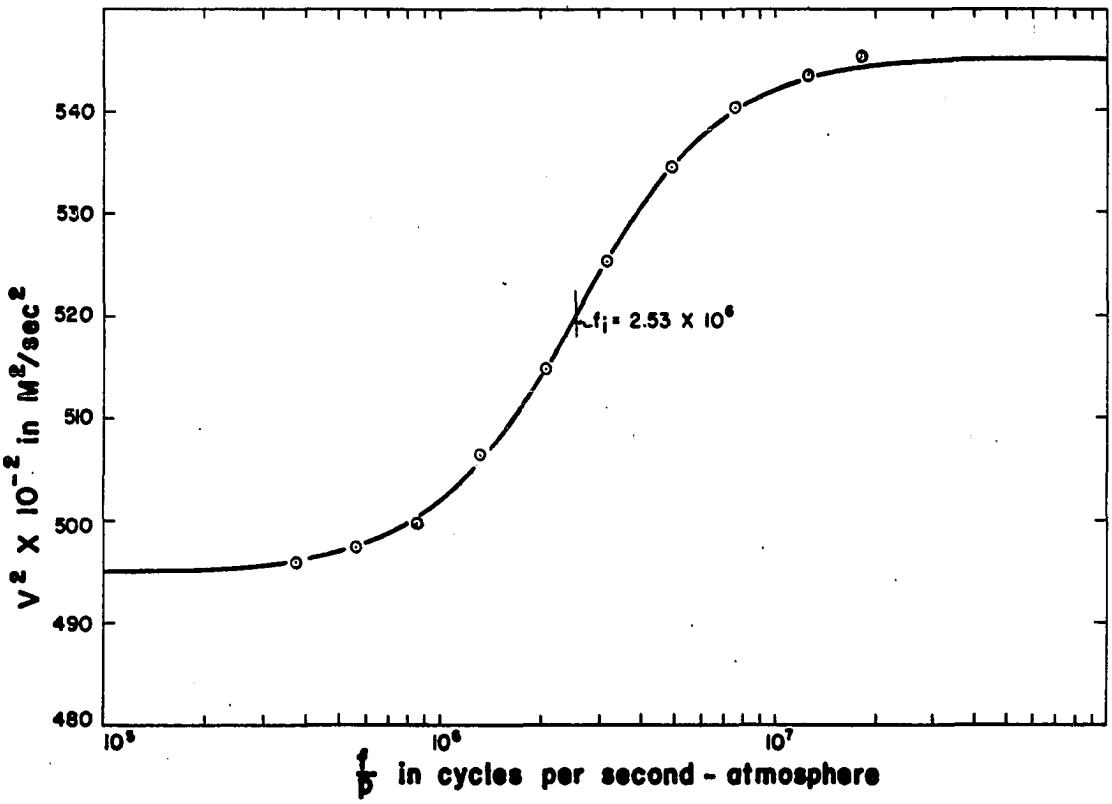

Fig. 11 Velocity dispersion in 51.2% CH_2F_2 - 48.8% CHF_3 at 299.0° K.

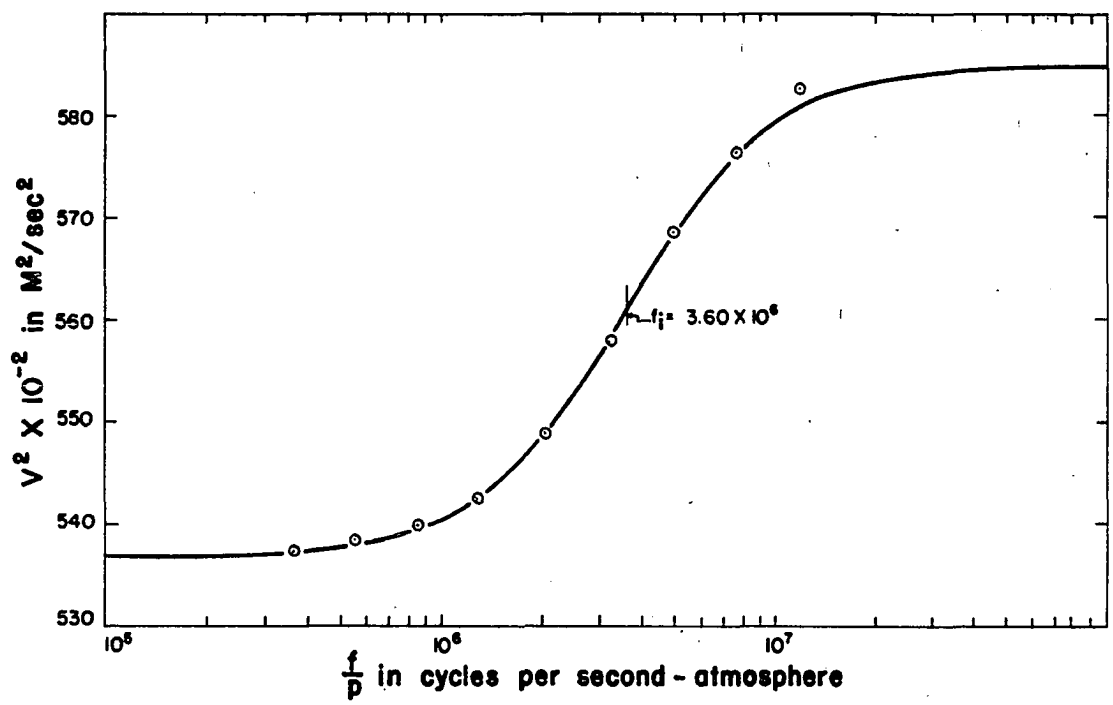

Fig. 12 Velocity dispersion in 73.9% CH_2F_2 - 26.1% CHF_3 at 299.2° K.

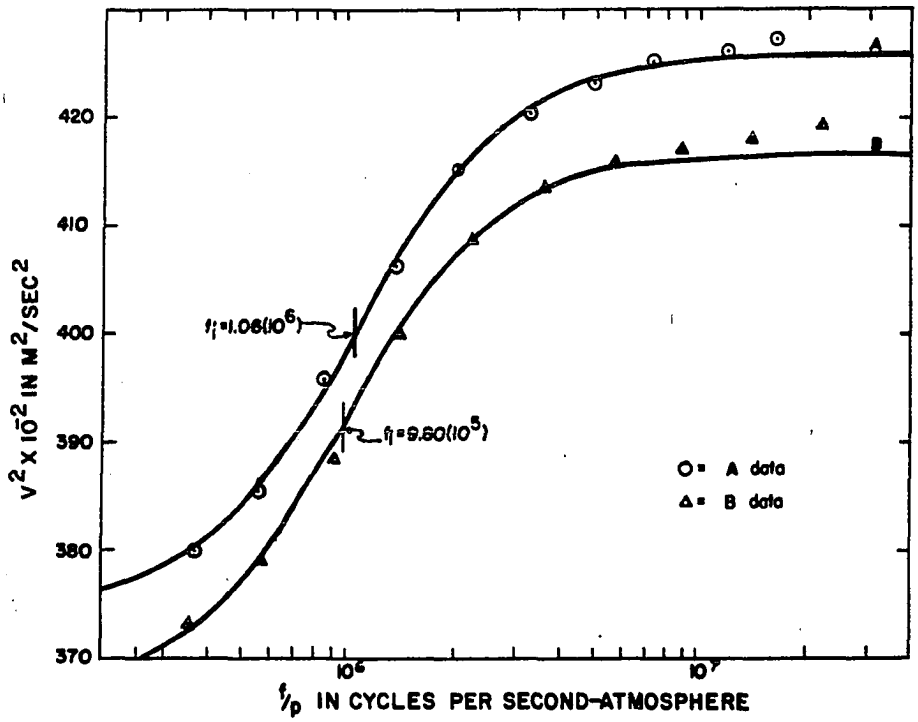

Fig. 13 Curve A - velocity dispersion in 27.5% CH_2F_2 - 72.5% CF_4 at 300.0° K.
Curve B - velocity dispersion in 25.2% CH_2F_2 - 74.8% CF_4 at 296.8° K.

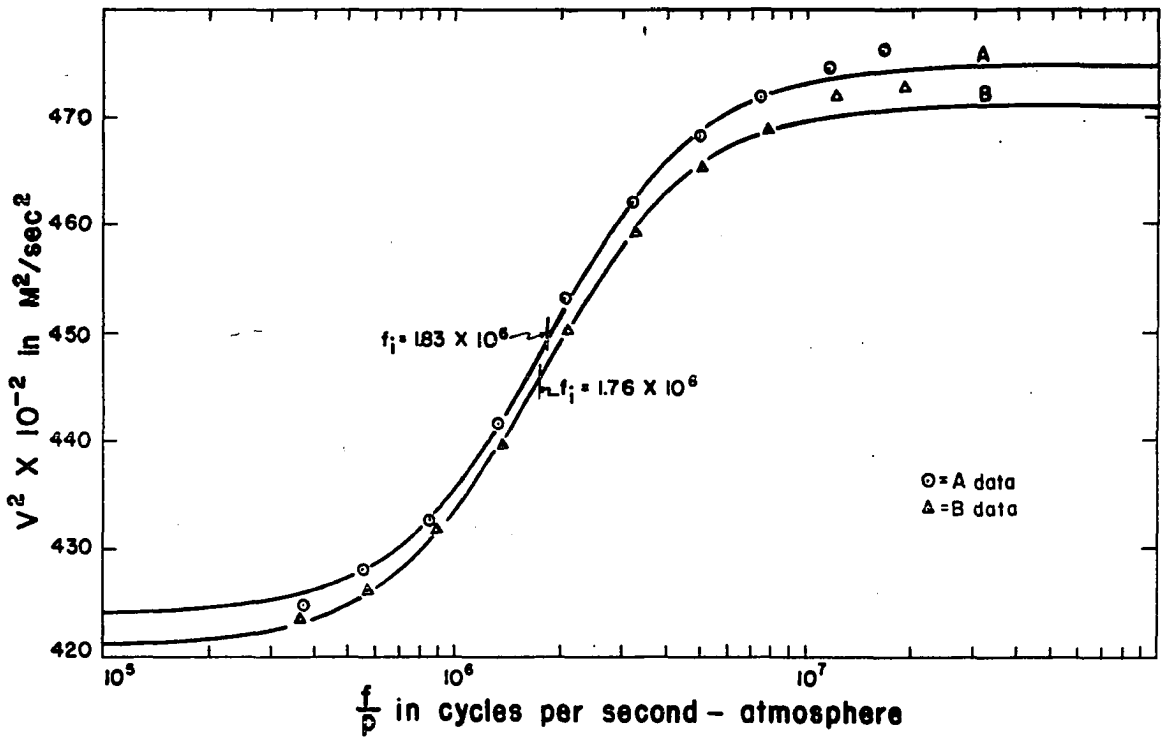

Fig. 14 Curve A - velocity dispersion in 50.4% CH_2F_2 - 49.6% CF_4 at 299.2° K.
Curve B - velocity dispersion in 49.9% CH_2F_2 - 50.1% CF_4 at 297.3° K.

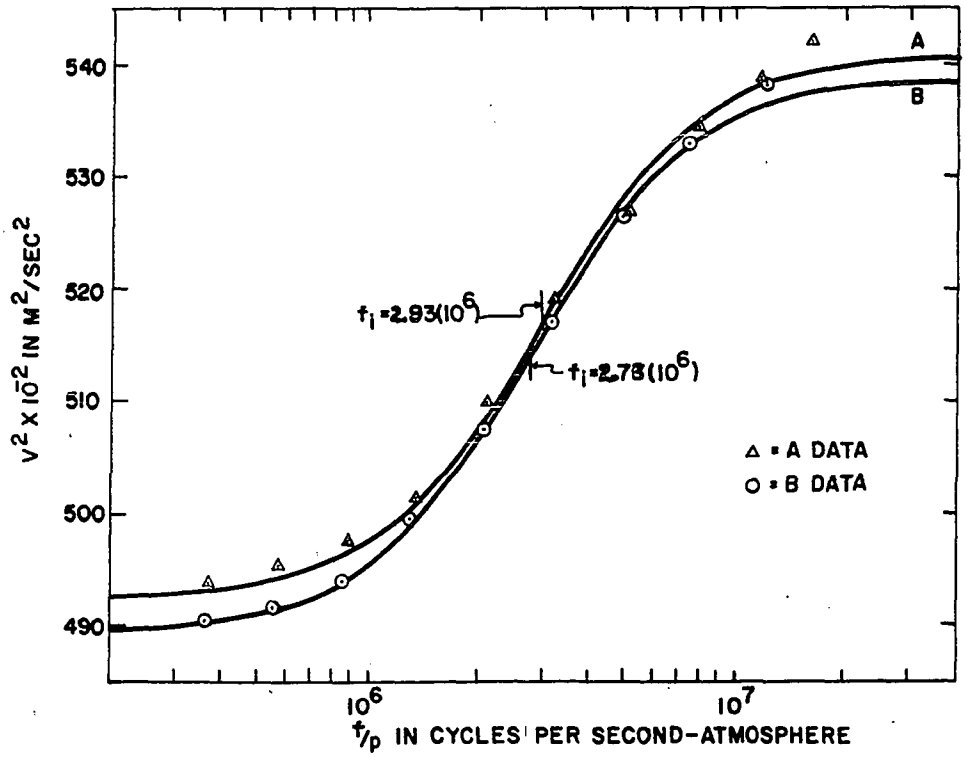

Fig. 15 Curve A - velocity dispersion in 75.2% CH_2F_2 - 24.8% CF_4 at 297.3° K.
Curve B - velocity dispersion in 73.8% CH_2F_2 - 26.2% CF_4 at 298.6° K.

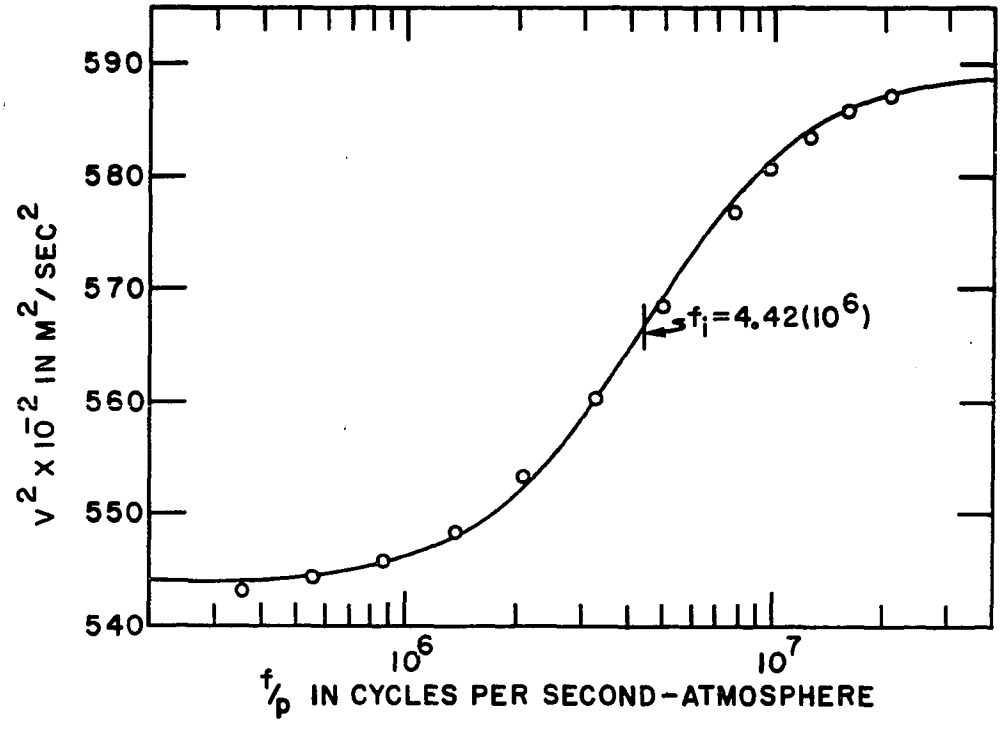

Fig. 16 Velocity dispersion in 90.0% CH_2F_2 - 10.0% CF_4 at 295.6° K.

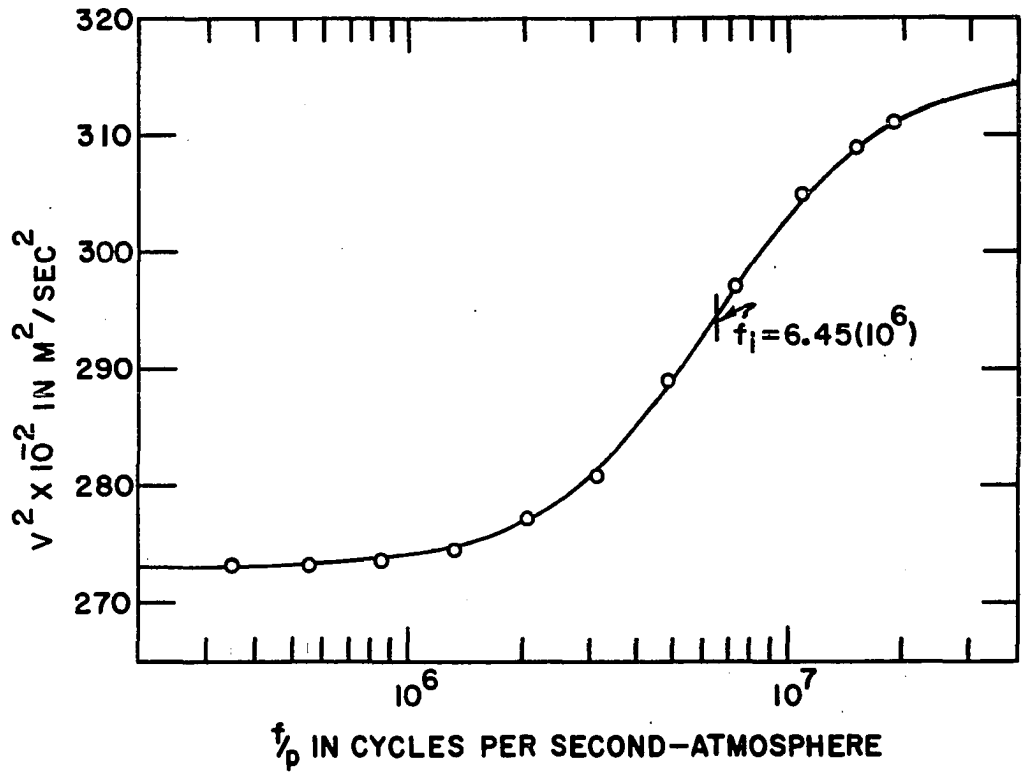

Fig. 17 Velocity dispersion in 24.3% CH_2F_2 - 75.7% CCl_2F_2 at 296.4° K.

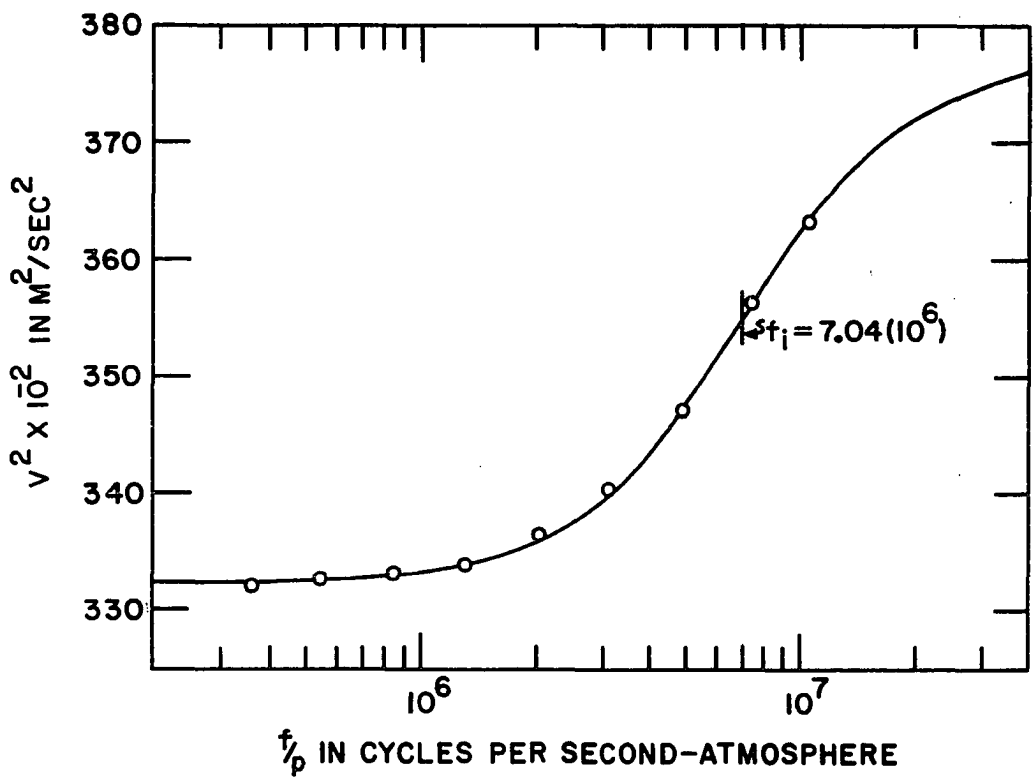

Fig. 18 Velocity dispersion in 49.0% CH_2F_2 - 51.0% CCl_2F_2 at 296.6° K.

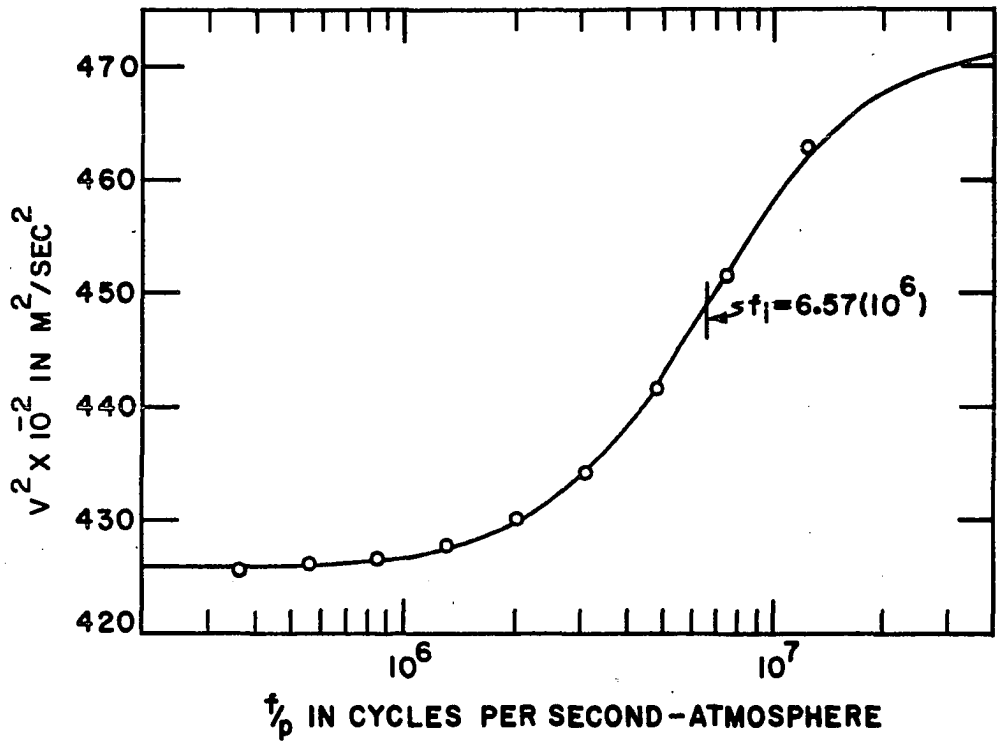

Fig. 19 Velocity dispersion in 74.2% CH_2F_2 - 25.8% CCl_2F_2 at 297.3° K.

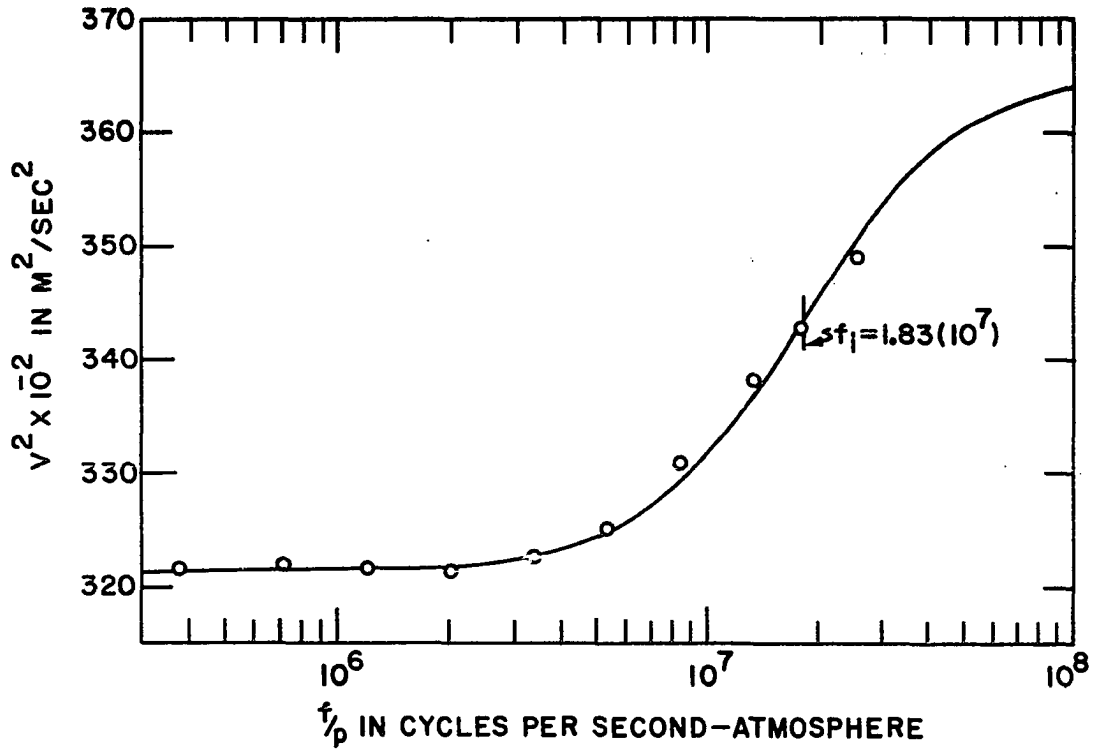

Fig. 20 Velocity dispersion in 24.7% CH_2F_2 - 75.3% $CHCl_2F$ at 297.7° K.

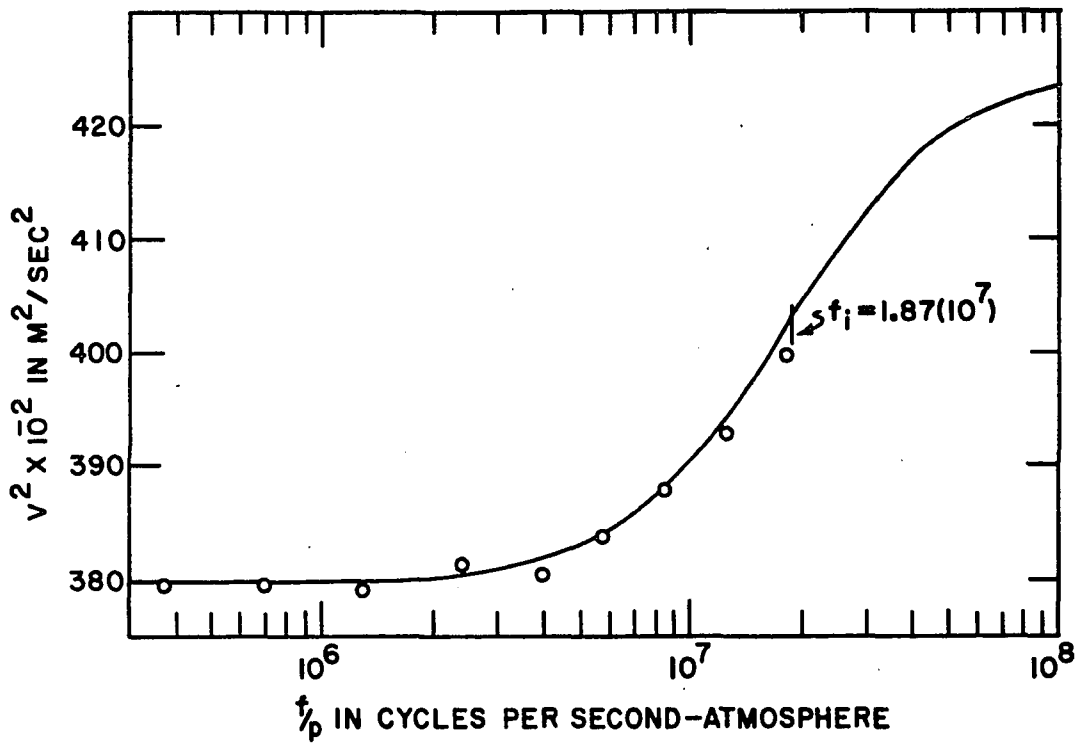

Fig. 21 Velocity dispersion in 50.1% CH_2F_2 - 49.9% $CHCl_2F$ at 296.7° K.

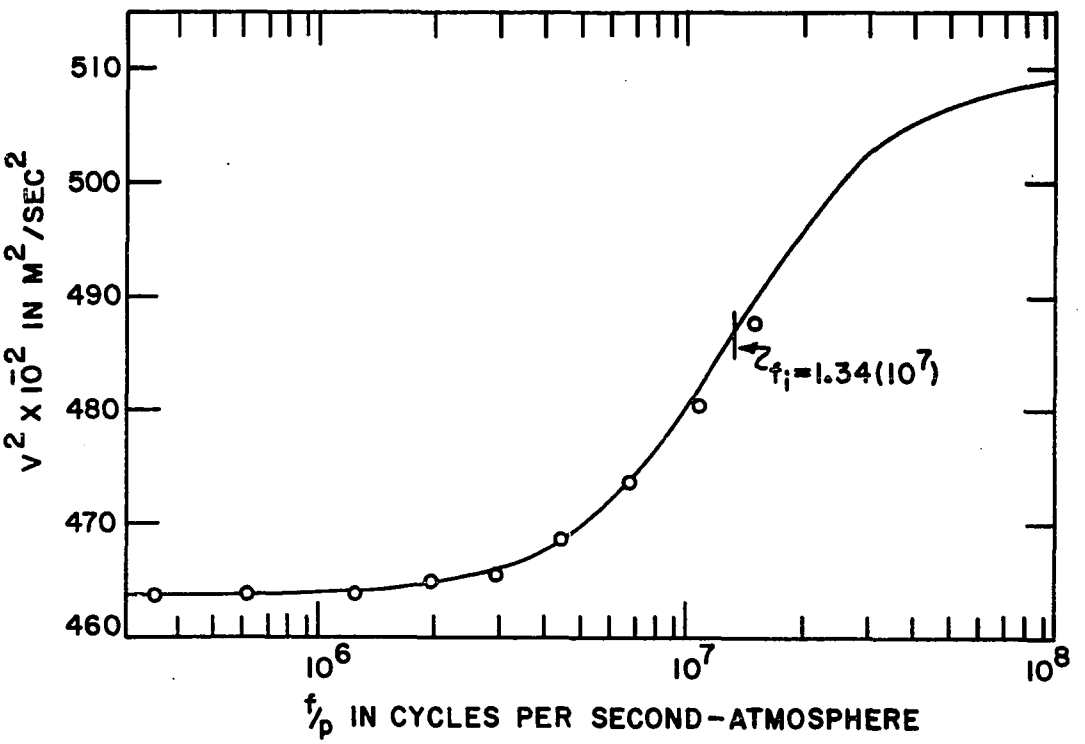

Fig. 22 Velocity dispersion in 75.0% CH_2F_2 - 25.0% $CHCl_2F$ at 297.6° K.

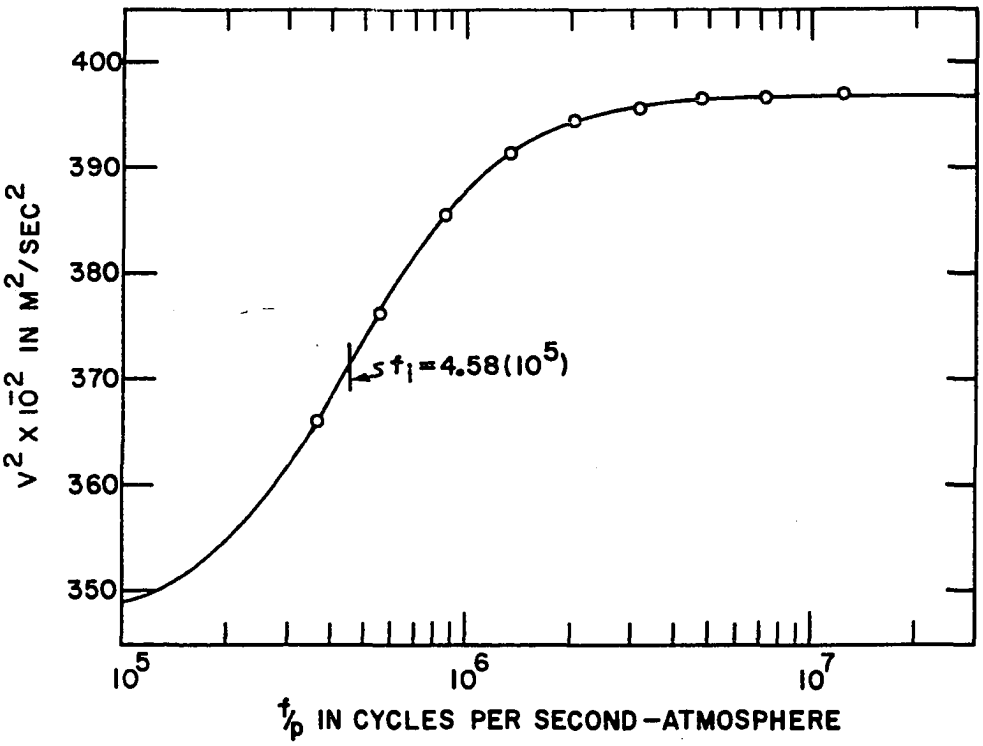

Fig. 23 Velocity dispersion in 26.7% CHF_3 - 73.3% CF_4 at 297.7° K.

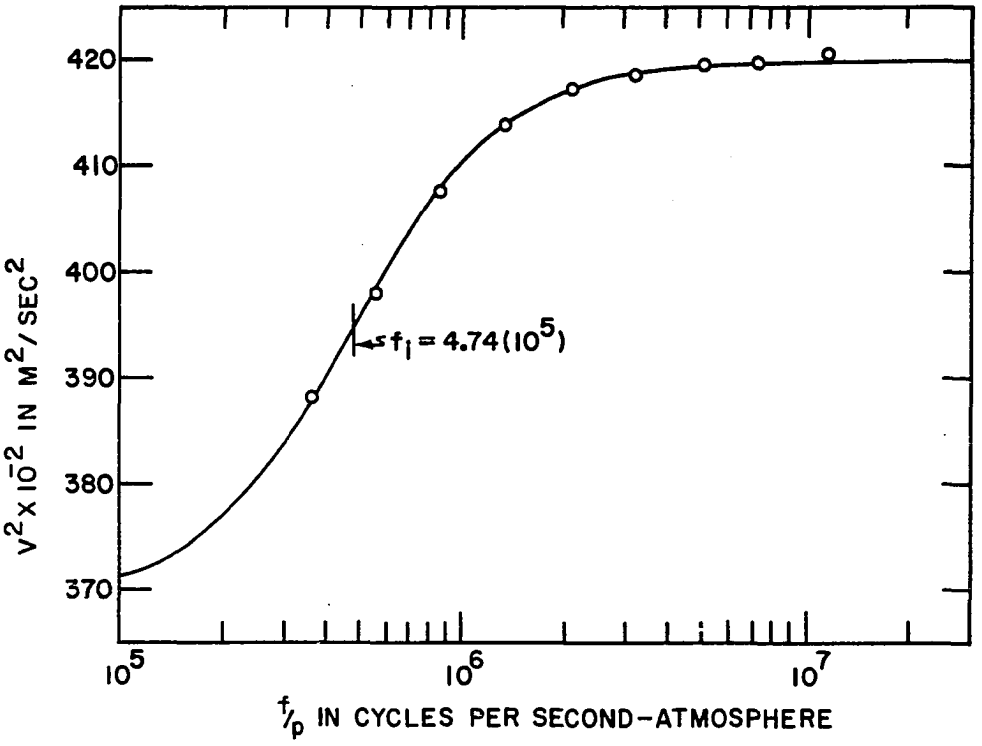

Fig. 24 Velocity dispersion in 51.7% CHF_3 - 48.3% CF_4 at 298.0° K.

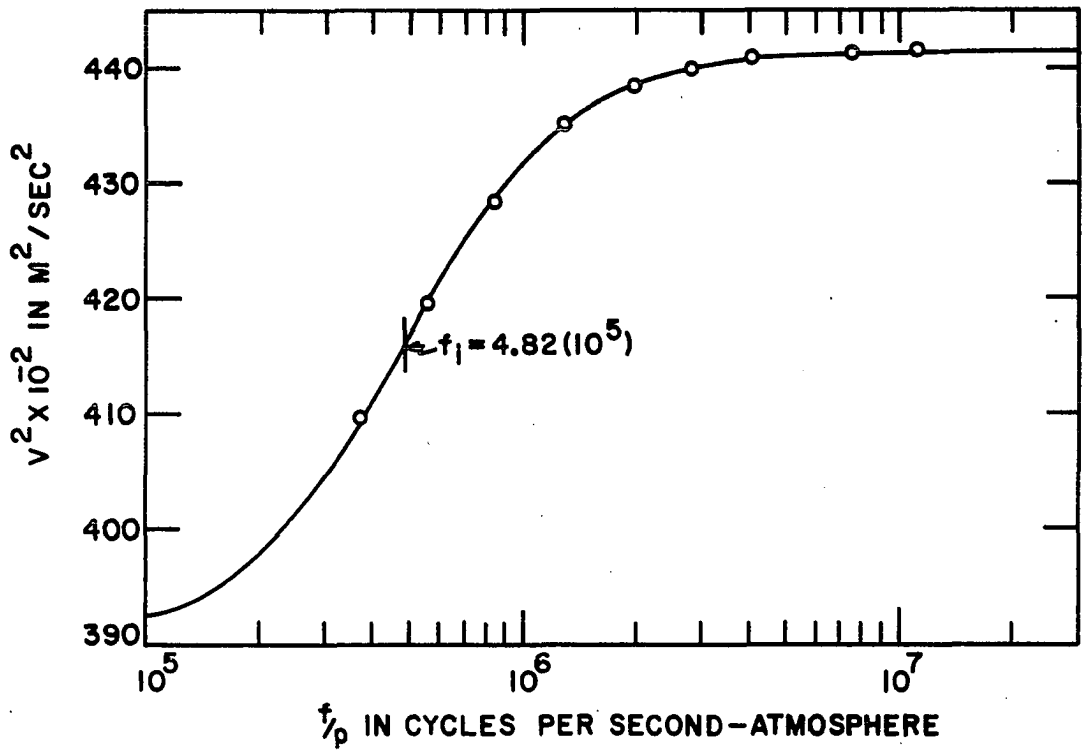

Fig. 25 Velocity dispersion in 74.9% CHF_3 - 25.1% CF_4 at 296.6° K.

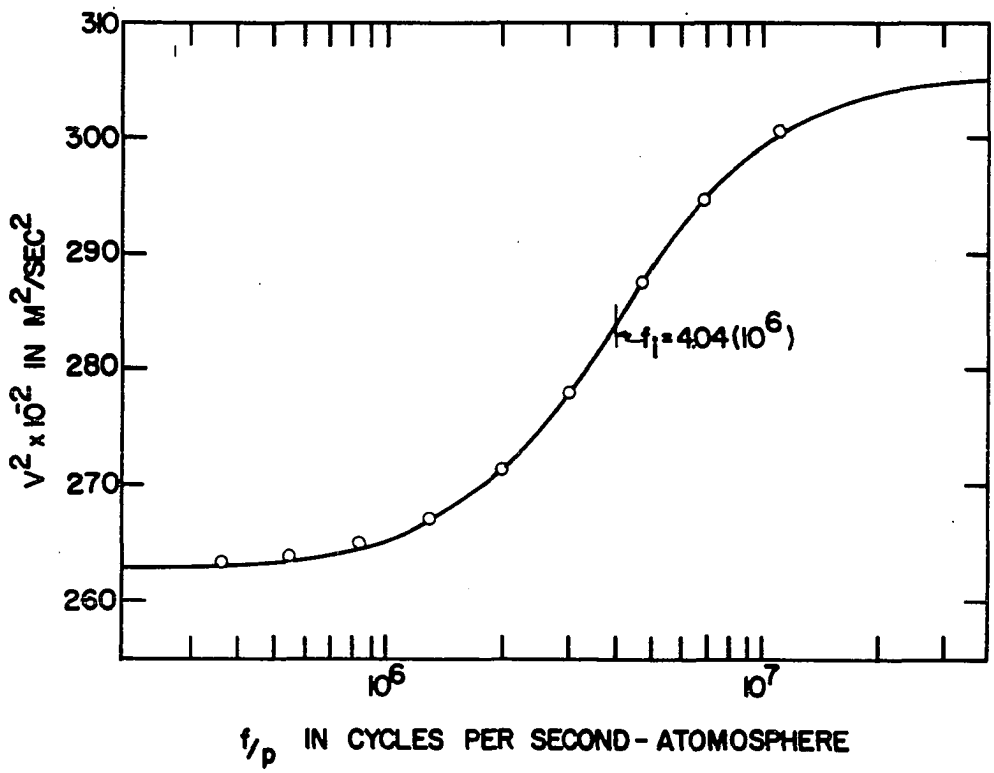

Fig. 26 Velocity dispersion in 25.0% CHF_3 - 75.0% CCl_2F_2 at 298.0° K.

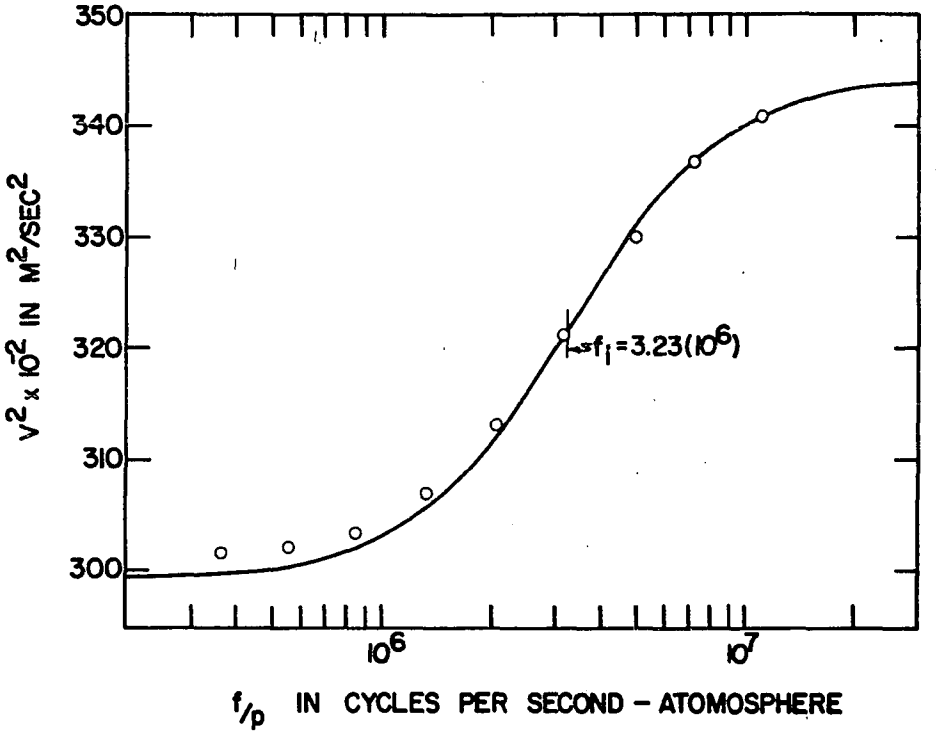

Fig. 27 Velocity dispersion in 49.0% CHF_3 - 51.0% CCl_2F_2 at 298.2° K.

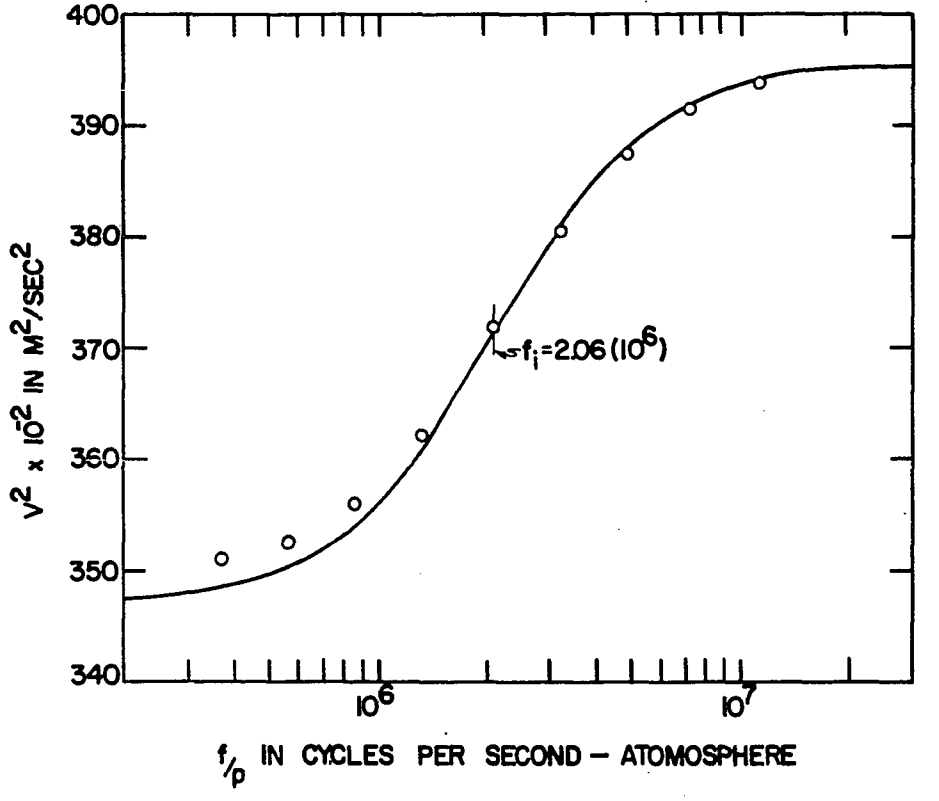

Fig. 28 Velocity dispersion in 73.1% CHF_3 - 26.9% CCl_2F_2 at 298.6° K.

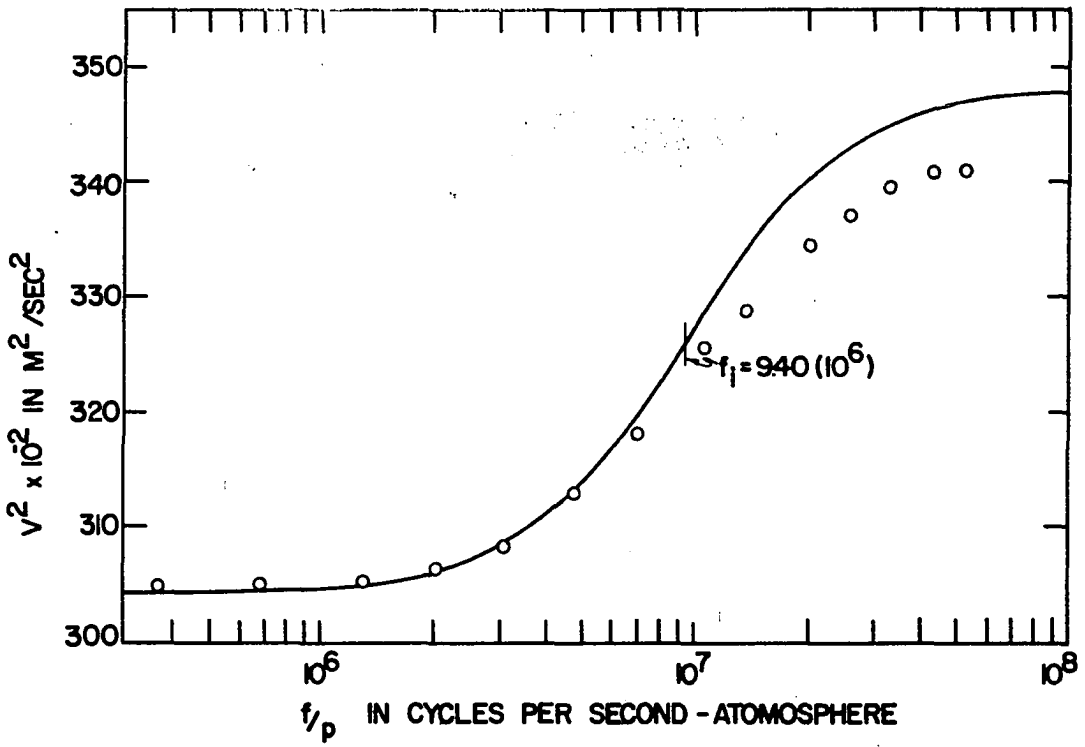

Fig. 29 Velocity dispersion in 25.4% CHF_3 - 74.6% $CHCl_2F$ at 297.3° K.

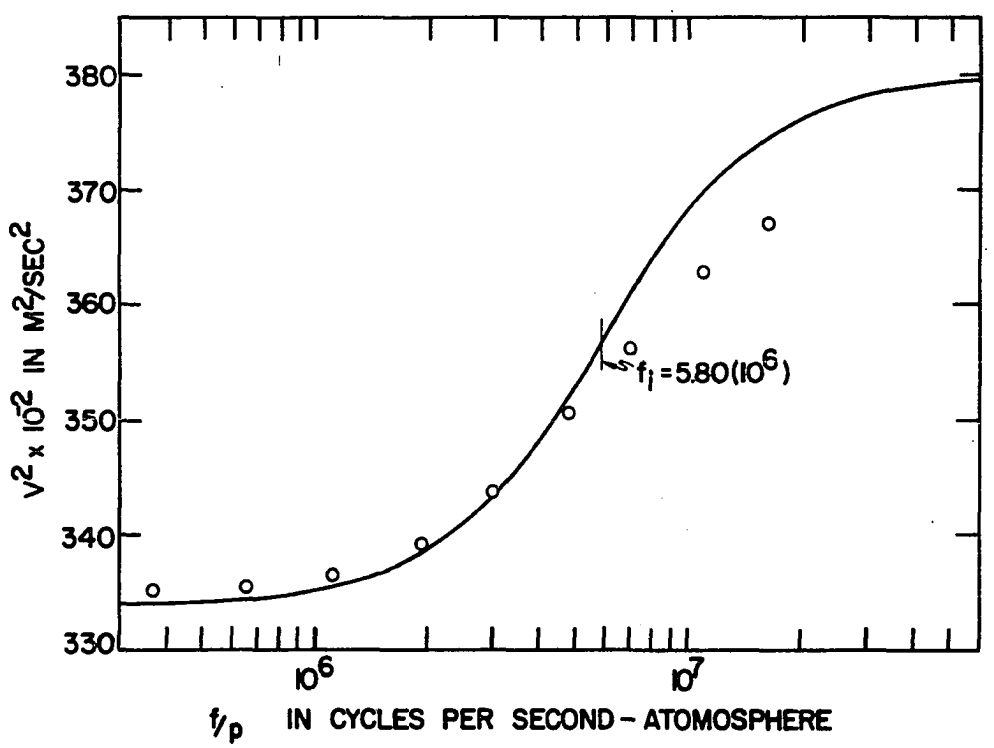

Fig. 30 Velocity dispersion in 49.8% CHF_3 - 50.2% $CHCl_2F$ at 296.6° K.

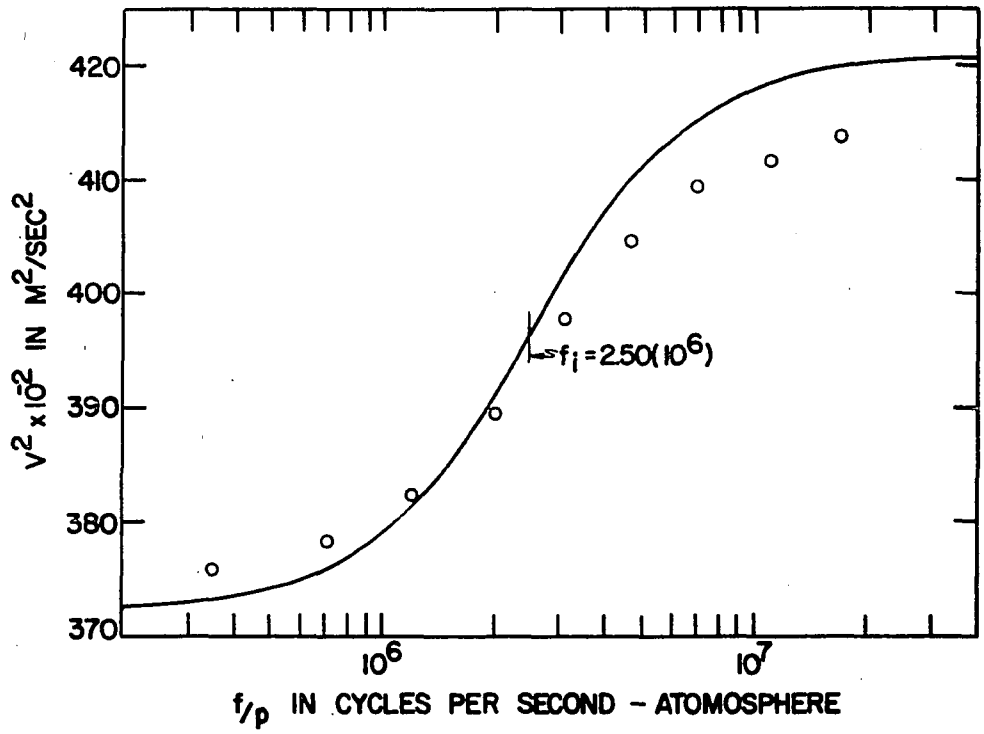

Fig. 31 Velocity dispersion in 75.4% CHF_3 - 24.6% $CHCl_2F$ at 296.6° K.

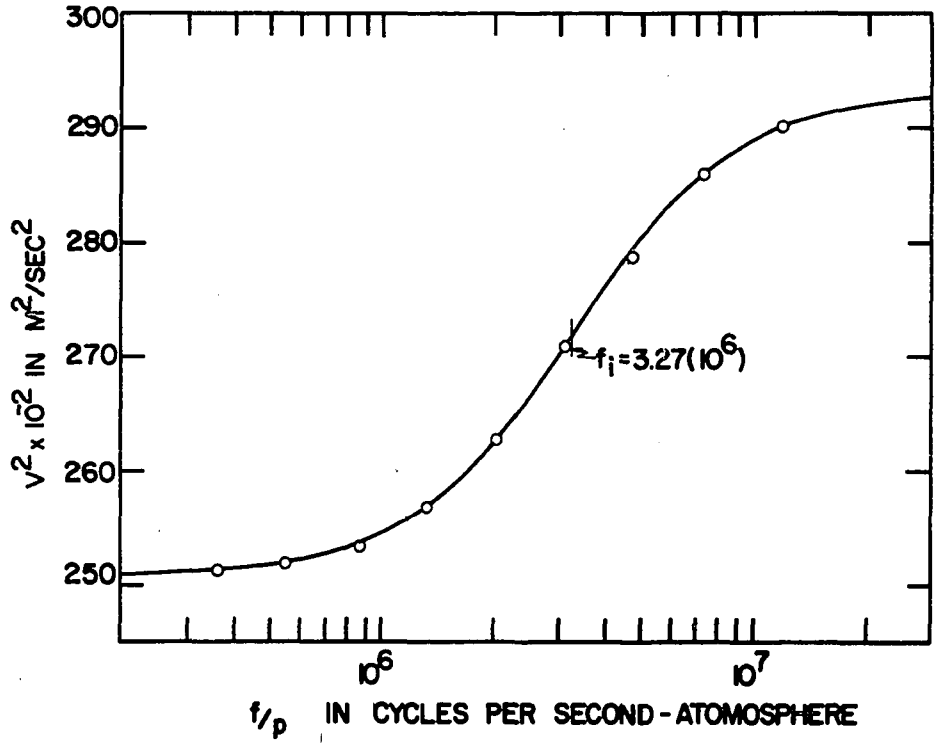

Fig. 32 Velocity dispersion in 24.0% CF_4 - 76.0% CCl_2F_2 at 298.8° K.

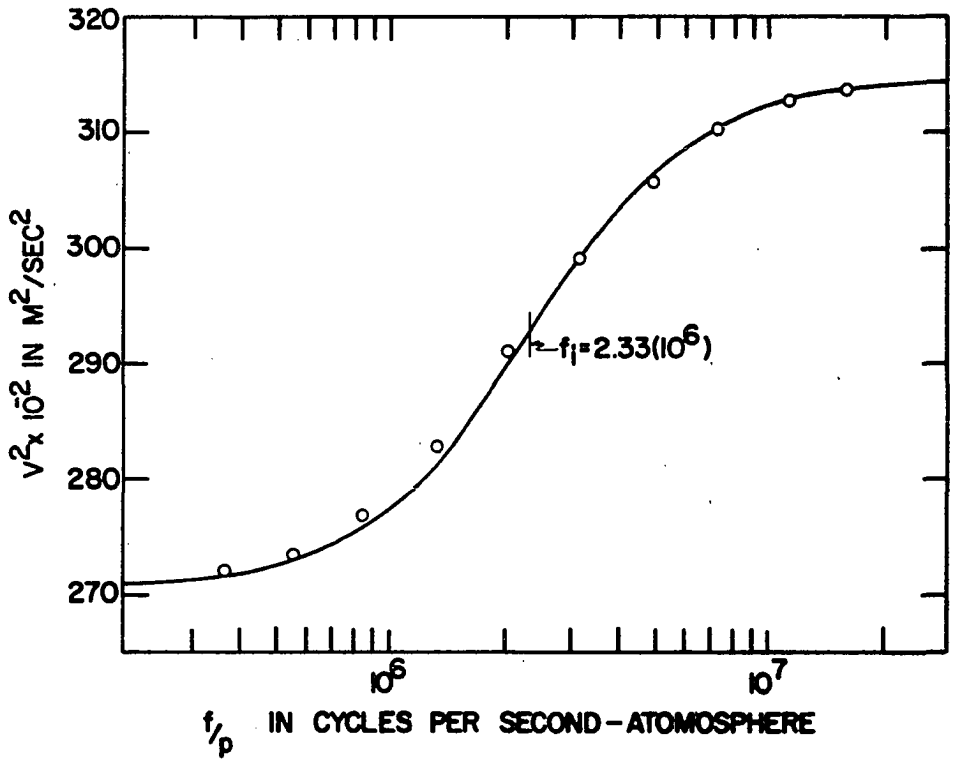

Fig. 33 Velocity dispersion in 49.5% CF_4 - 50.5% CCl_2F_2 at 297.1° K.

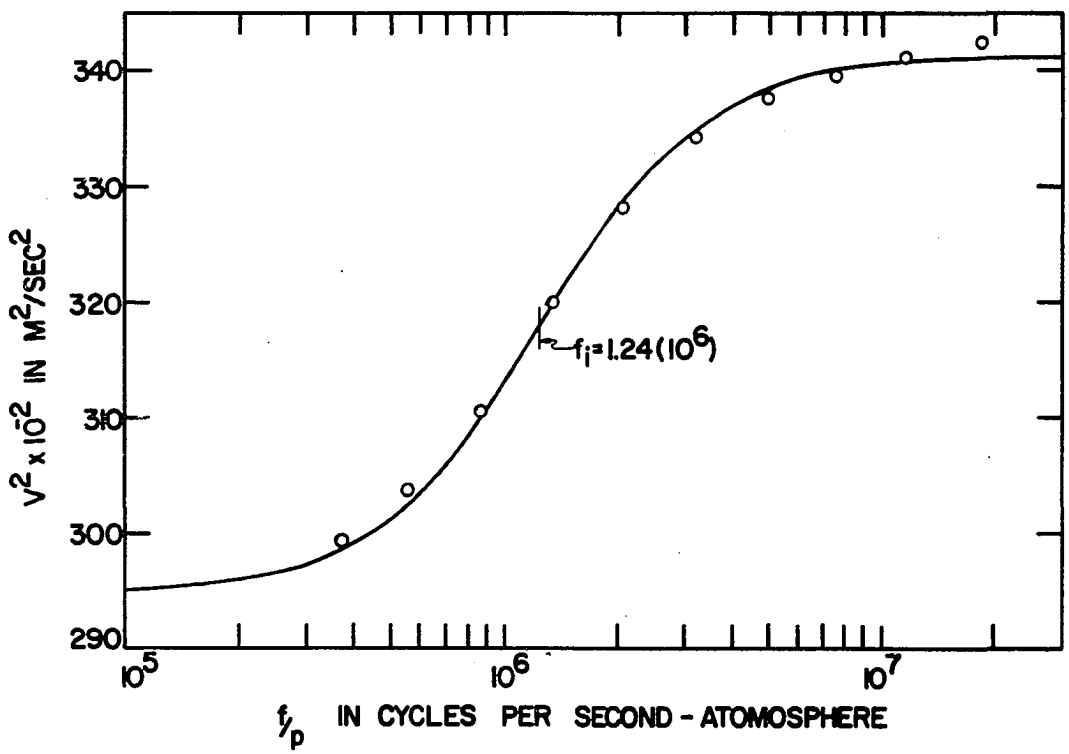

Fig. 34 Velocity dispersion in 74.3% CF_4 - 25.7% CCl_2F_2 at 296.8° K.

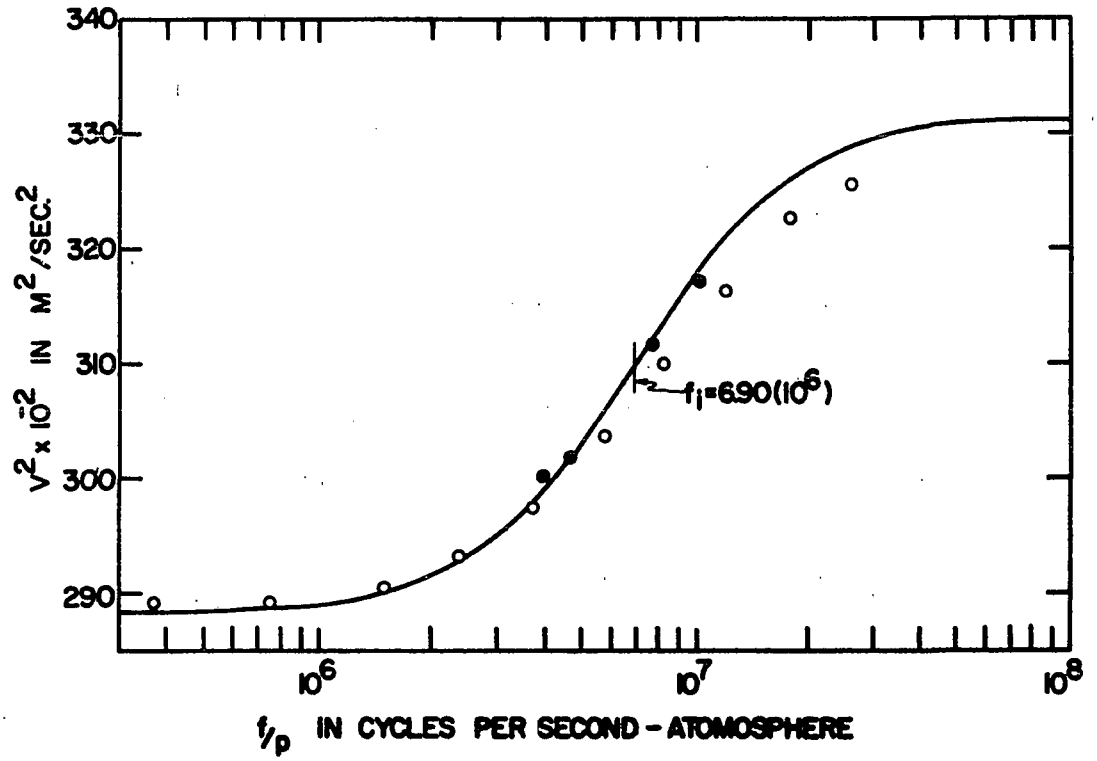

Fig. 35 Velocity dispersion in 26.0% CF_4 - 74.0% $CHCl_2F$ at 296.3° K.

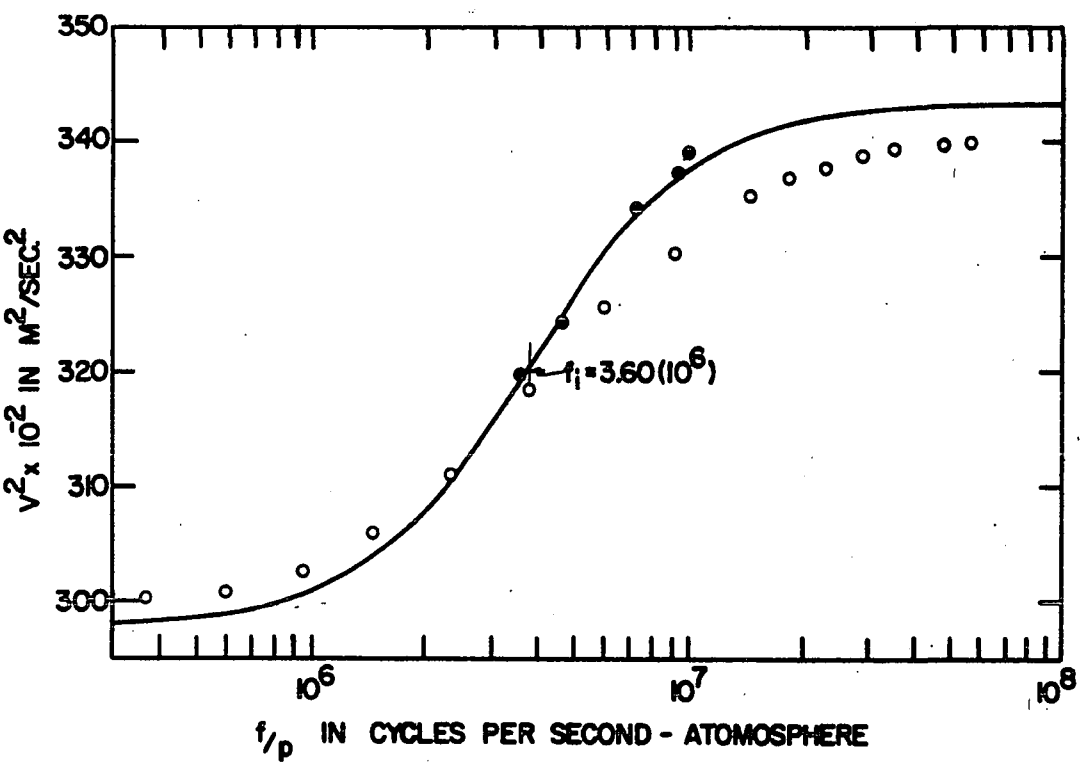

Fig. 36 Velocity dispersion in 50.1% CF_4 - 49.9% $CHCl_2F$ at 295.5° K.

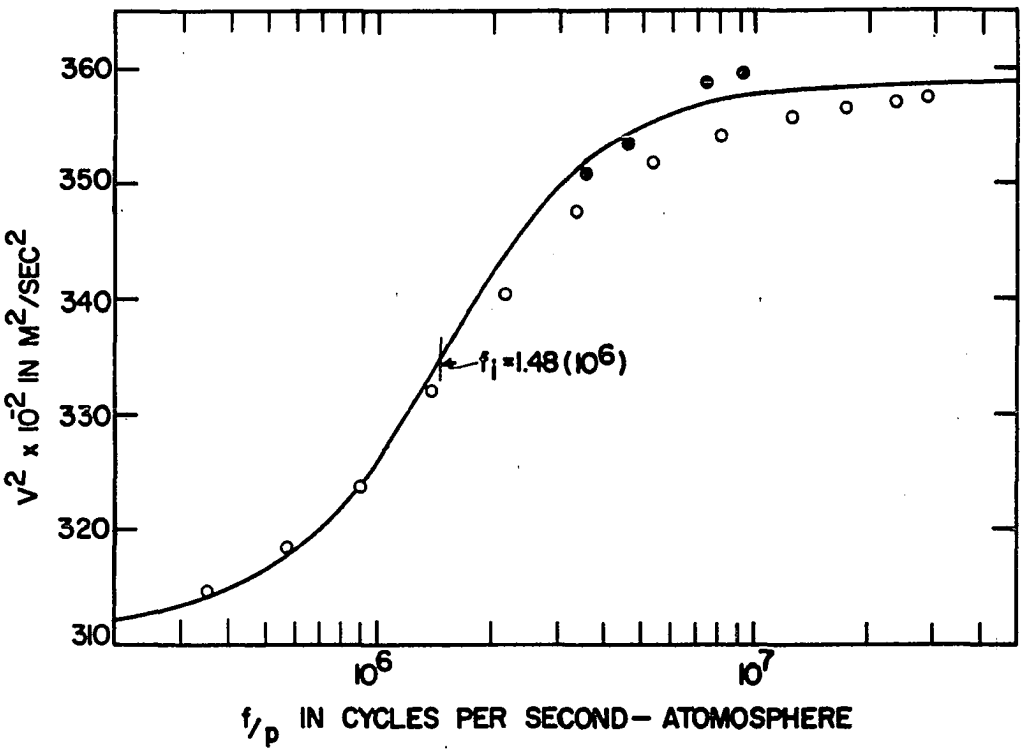

Fig. 37 Velocity dispersion in 75.2% CF_4 - 24.8% $CHCl_2F$ at 296.6° K.

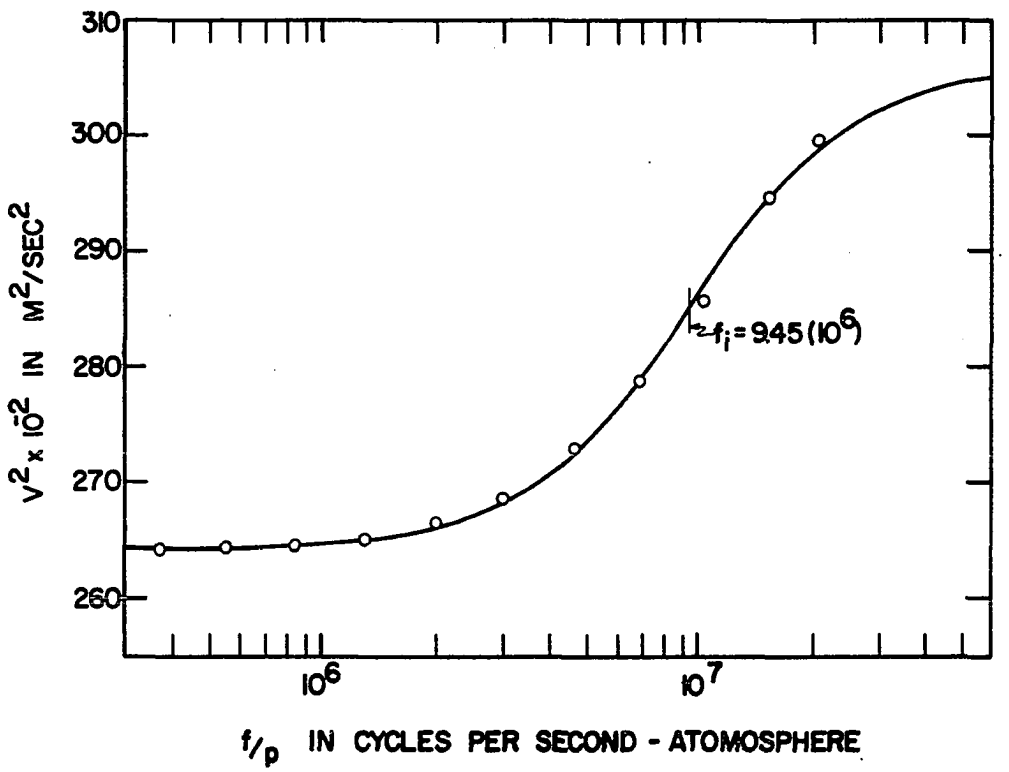

Fig. 38 Velocity dispersion in 26.0% CCl_2F_2 - 74.0% $CHCl_2F$ at 296.8° K.

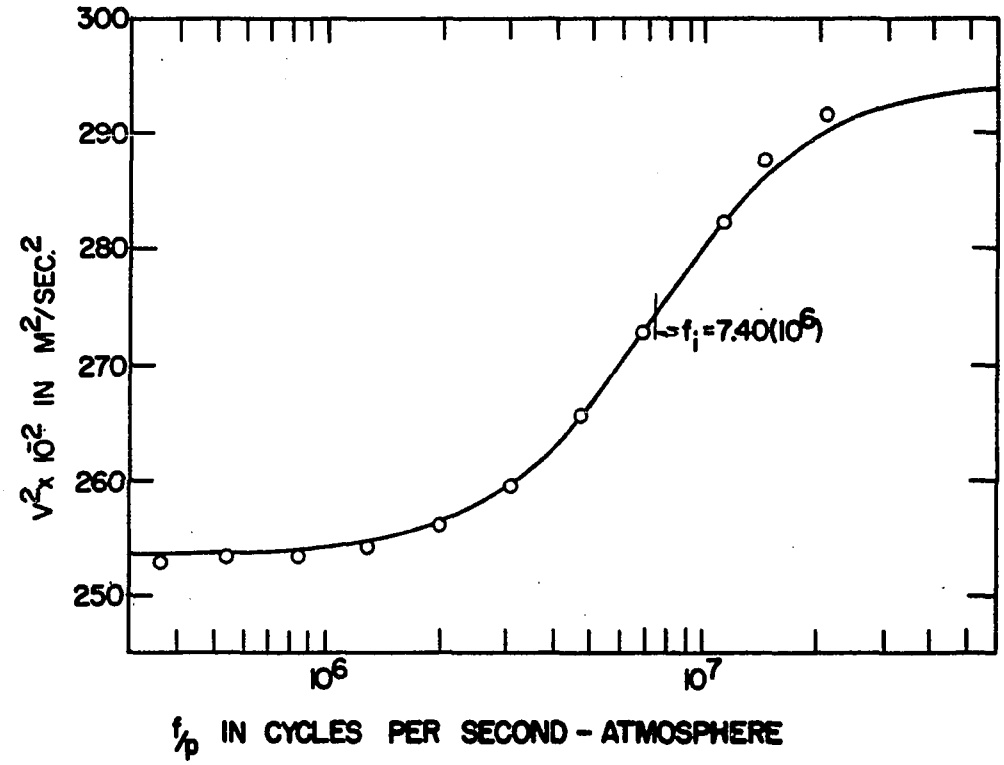

Fig. 39 Velocity dispersion in 50.0% CCl_2F_2 - 50.0% $CHCl_2F$ at 297.7° K.

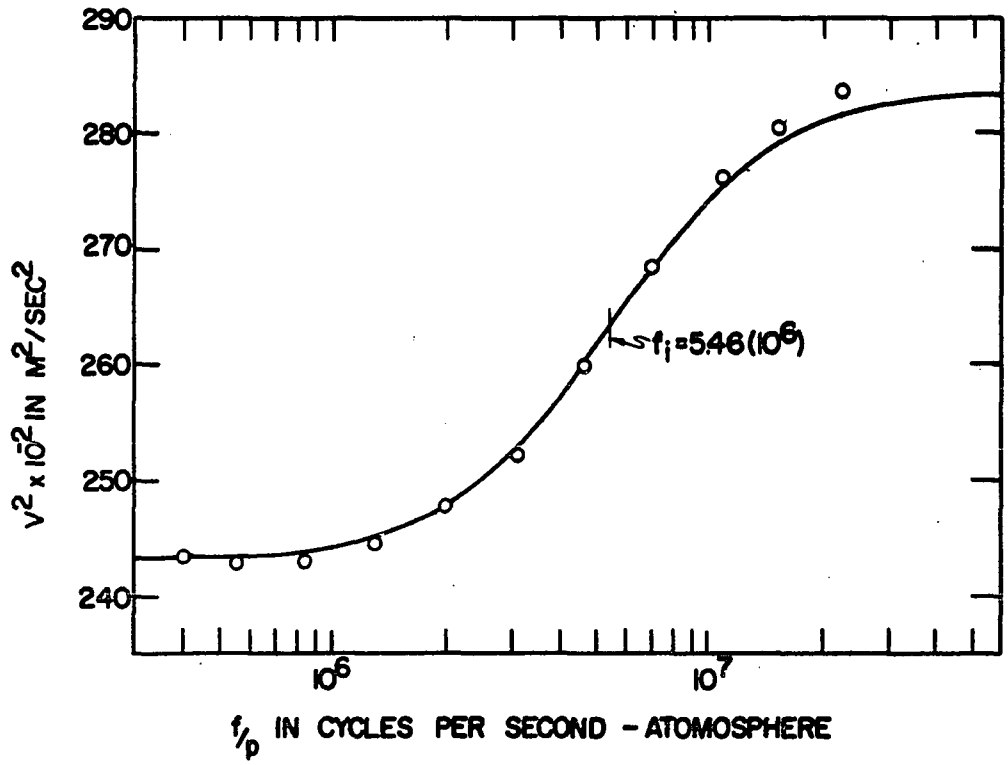

Fig. 40 Velocity dispersion in 74.5% CCl_2F_2 - 25.5% $CHCl_2F$ at 297.7° K.

However, as the pressure is reduced, the points tend to deviate from the curve. This could suggest that more than one relaxation time obtains. An effort was made to fit the data to the double dispersion expression (Equation 13) using various combinations of the vibrational specific heats of the two gases for C_1 and C_2. For no values of τ_1 and τ_2 were the data compatible with the calculated theoretical curves. The conclusion to be drawn here is that multiple dispersion is not the reason for the deviations from the theoretical curves.

Other possible explanations are that the concentration of the mixture changes as the pressure is reduced or that a chemical reaction takes place. The latter is extremely unlikely since the molecules considered here are very stable. The concentration variation then remains to be considered.

A possible cause for such a variation could be the differing adsorption properties of the mixture components. $CHCl_2F$ is known to adhere more readily to the surfaces of the chamber than the other gases considered here. This would indicate there is a greater concentration of $CHCl_2F$ on the surfaces than there is spatially within the chamber. When the pressure is reduced only the spatial gas is removed. Some of the surface molecules must then become spatial molecules in order to reach a new equilibrium at

the new pressure. This results in a new spatial concentration which is richer in $CHCl_2F$. Since $CHCl_2F$ is heavier than either CHF_3 or CF_4, the new effective molecular weight is greater and, consequently, the velocity should be lower.

In an effort to obtain experimental verification that a concentration variation was taking place, the mixture constituents were admitted to the system in the usual manner, only at a lower total pressure. The solid points on the CF_4-$CHCl_2F$ curves correspond to total filling pressures ranging from about 3 cm. Hg. to about 8 cm. Hg. These points were taken individually, i.e. each point corresponds to a separate filling. As is evident, these points are all higher than the original points and compare quite favorably with the theoretical curve.

A similar experiment was attempted with the CHF_3-$CHCl_2F$ mixtures. The results, however, were not conclusive and are not shown. The problem here lies in reproducing the exact concentration of the original mixture. Since the molecular weights of CHF_3 and $CHCl_2F$ differ significantly, V^2 in these mixtures will be more sensitive to variations in concentration than in the CF_4-$CHCl_2F$ mixtures. For this reason there was considerable scatter in the points and no conclusions could be drawn. The theoretical curves for the CHF_3-$CHCl_2F$ have been fitted

to the existing data, with most weight given to the data taken at high pressures.

Whether a concentration variation is actually taking place is subject to considerable question. It is possible that some other mechanism is responsible for the observed behavior. However, if one does put credence in the points taken at low filling pressures in the CF_4-$CHCl_2F$ mixtures, a change in concentration does seem plausible. This analysis in no way verifies the proposed reason for a variation in concentration, but only shows the possible existence of such a mechanism.

In the remaining figures, single dispersion is quite evident. The relaxation times obtained for the pure gases are presented in Table 3. The relaxation times for the mixtures are presented in Tables 4 and 5. These tables also

Table 3. C_o, f_i, τ, and τ^{-1} for the pure gases

Gas	C_o (cal/mole-deg)	$f_i(10^{-6})$ (sec^{-1})	$\tau(10^7)$ (sec)	$\tau^{-1}(10^{-7})$ (sec^{-1})
CH_2F_2	8.22	5.50	.399	2.50
CHF_3	10.61	.466	6.08	.164
CF_4	12.65	.412	8.20	.122
CCl_2F	14.50	4.65	.833	1.20
$CHCl_2F$	12.69	12.7	.267	3.75

Table 4. C_o, f_i, τ, τ^{-1}, and $(\tau_{AB}^{-1} + \tau_{BA}^{-1})$ of mixtures for which the requirements of Equation 59 are satisfied

Gas A	Gas B	% Gas A	C_o (cal/ mole-deg)	$f_i(10^{-6})$ (sec^{-1})	$\tau(10^7)$ (sec)	$\tau^{-1}(10^{-7})$ (sec^{-1})	$(\tau_{AB}^{-1} + \tau_{BA}^{-1})(10^{-7})$ (sec^{-1})
CH_2F_2	CCl_2F_2	24.3	12.92	6.45	.535	1.87	5.61
"	"	49.0	11.38	7.04	.432	2.32	5.61
"	"	74.2	9.82	6.57	.399	2.50	5.47
CH_2F_2	$CHCl_2F$	24.7	11.55	18.3	.169	5.93	19.7
"	"	50.1	10.39	18.7	.148	6.74	20.7
"	"	75.0	9.32	13.4	.186	5.38	20.0
CHF_3	CF_4	26.7	12.09	.458	7.05	.142	.330
"	"	51.7	11.60	.474	6.54	.153	.323
"	"	74.9	11.10	.482	6.15	.163	.334
CHF_3	CCl_2F_2	25.0	13.52	4.04	.894	1.119	2.31
"	"	49.0	12.61	3.23	1.043	.959	2.43
"	"	73.1	11.70	2.06	1.52	.659	2.47
CF_4	CCl_2F_2	24.0	14.06	3.27	1.15	.871	.93
"	"	49.5	13.57	2.33	1.56	.643	1.23
"	"	74.3	13.07	1.24	2.82	.355	1.09
CCl_2F_2	$CHCl_2F$	26.0	13.08	9.45	.370	2.71	2.98
"	"	50.0	13.56	7.40	.490	2.04	3.22
"	"	74.5	14.01	5.46	.685	1.46	2.89

Table 5. C_o, f_i, τ, τ^{-1}, and $(\tau_{AB}^{-1} + \tau_{BA}^{-1})$ for mixtures not satisfying the requirements of Equation 59

Gas A	Gas B	% Gas A	C_o (cal/mole-deg)	$f_i(10^{-6})$ (sec^{-1})	$\tau(10^7)$ (sec)	$\tau^{-1}(10^{-7})$ (sec^{-1})	$(\tau_{AB}^{-1} + \tau_{BA}^{-1})(10^{-7})$ (sec^{-1})
CH_2F_2	CHF_3	26.7	10.04	1.425	1.88	.532	1.36
"	"	51.2	9.43	2.53	.996	1.004	1.23
"	"	73.9	8.88	3.60	.659	1.52	.72
CH_2F_2	CF_4	25.2	11.49	.980	3.13	.319	.486
"	"	27.5	11.48	1.06	2.89	.346	.462
"	"	49.9	10.40	1.76	1.58	.633	-.085
"	"	50.4	10.43	1.83	1.52	.657	-.038
"	"	73.8	9.41	2.73	.921	1.09	-1.48
"	"	75.2	9.30	2.93	.847	1.19	-1.31
"	"	90.0	8.62	4.42	.521	1.92	-1.21
CHF_3	$CHCl_2F$	25.4	12.12	9.40	.344	2.91	4.27
"	"	49.8	11.60	5.80	.534	1.87	3.55
"	"	75.4	11.09	2.50	1.19	.844	2.82
CF_4	$CHCl_2F$	26.0	12.58	6.90	.487	2.16	.514
"	"	50.1	12.63	3.60	.936	1.07	.418
"	"	75.2	12.59	1.48	2.27	.440	.758

show the reciprocal relaxation times as well as the effective specific heats at low frequencies. With the possible exception of the CHF_3-$CHCl_2F$ mixtures and the CF_4-$CHCl_2F$ mixtures, the probable errors of the relaxation times are estimated to be less than 5%. This figure was determined by shifting the theoretical velocity curves along the abscissa to determine the extreme values which the inflection frequencies could take, staying within the V^2 vs. f/P error range. The probable errors of the relaxation times in the CHF_3-$CHCl_2F$ and the CHF_3-$CHCl_2F$ mixtures are somewhat larger, due to the uncertainty of the experimental results, which appeared to suffer from systematic gas composition errors.

The reciprocal relaxation times are also presented graphically, as a function of concentration, in Figures 41 through 50. The dots on these curves represent the experimental reciprocal relaxation times for each concentration. The solid curves are calculated from Equation 59. Values for $(\tau_{AB}^{-1} + \tau_{BA}^{-1})$ were determined for each experimental concentration and the average of these was used in the calculation. No curve is shown for the CH_2F_2-CF_4 mixtures because some of the experimental values of $(\tau_{AB}^{-1} + \tau_{BA}^{-1})$ were physically impossible. Further discussion of this will follow.

The validity of the quadratic dependence of reciprocal

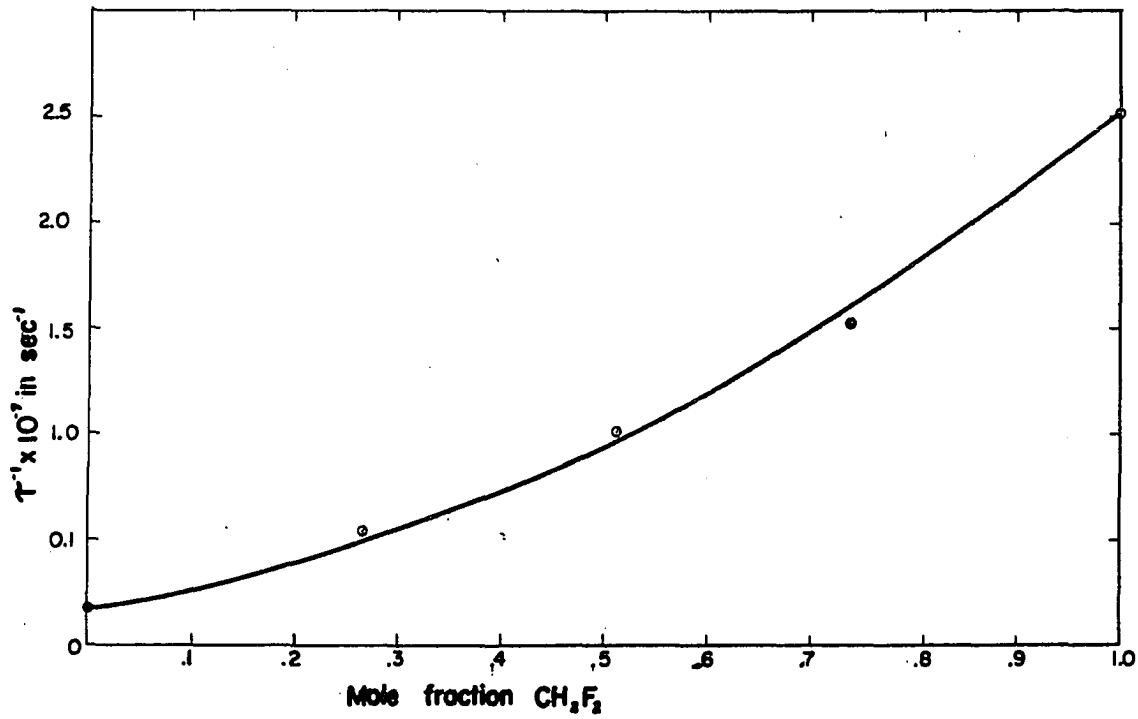

Fig. 41 Reciprocal relaxation time vs. concentration in CH_2F_2 - CHF_3 mixtures.

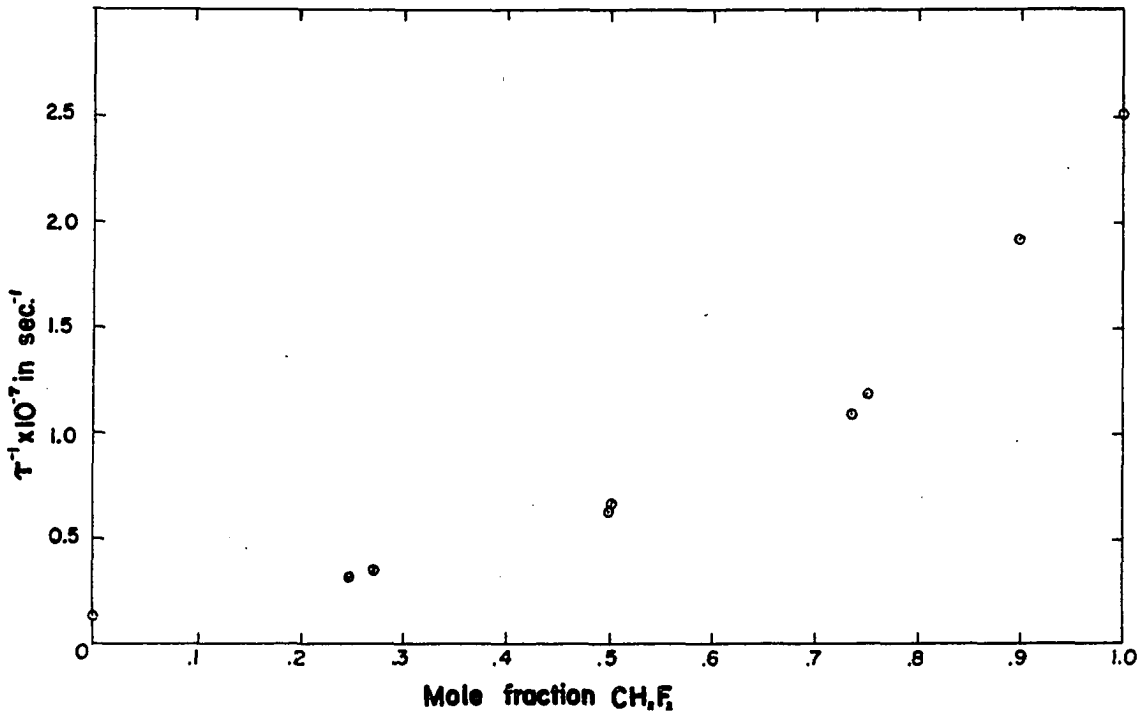

Fig. 42 Reciprocal relaxation time vs. concentration in CH_2F_2 - CF_4 mixtures.

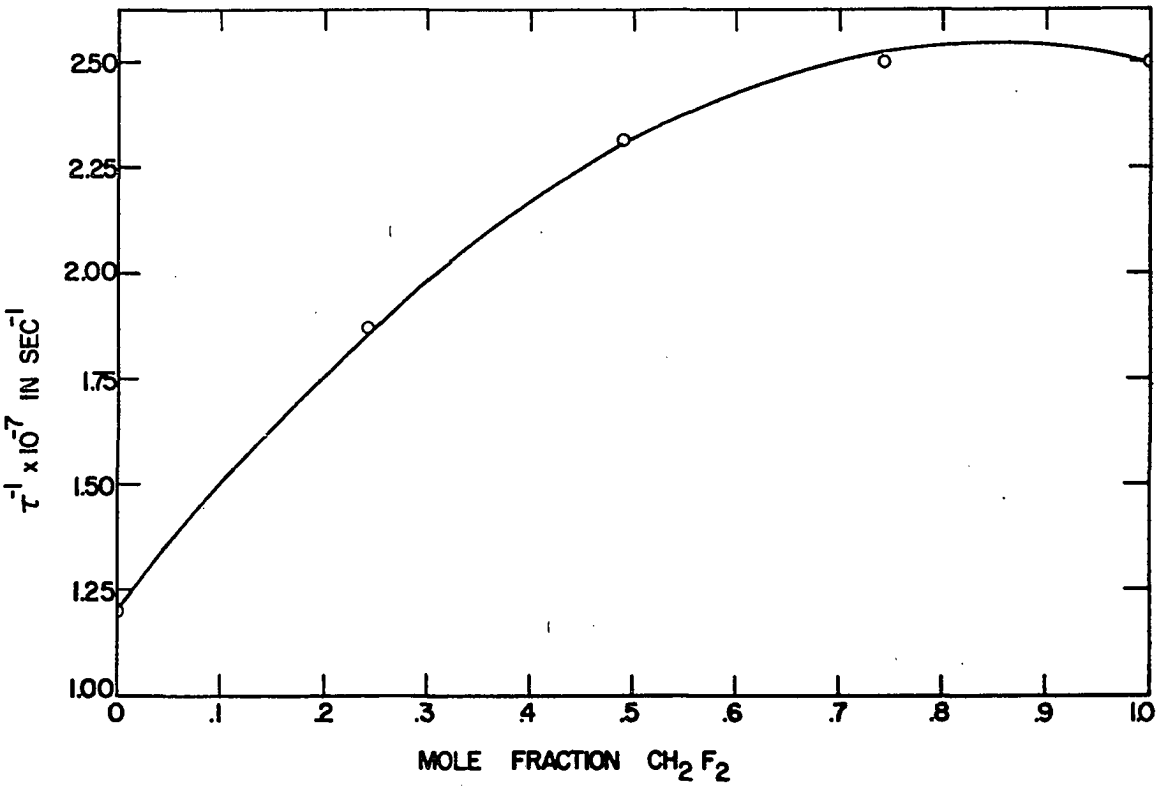

Fig. 43 Reciprocal relaxation time vs. concentration in CH_2F_2 - CCl_2F_2 mixtures.

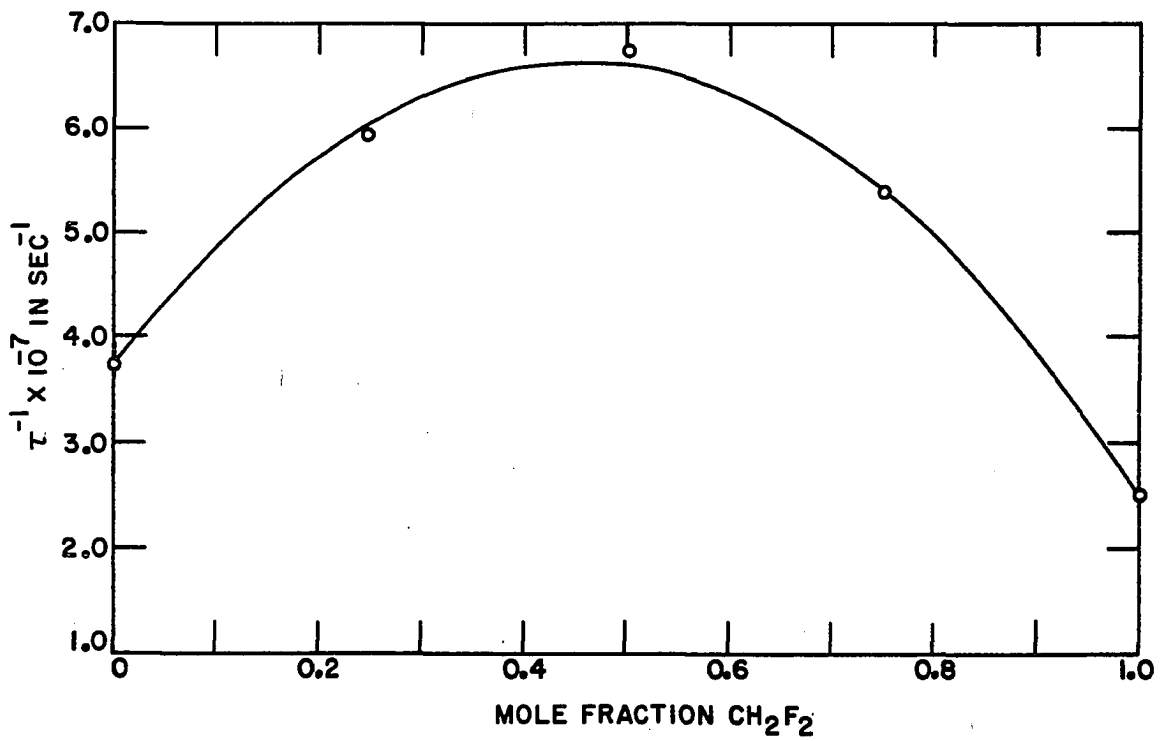

Fig. 44 Reciprocal relaxation time vs. concentration in CH_2F_2 - $CHCl_2F$ mixtures.

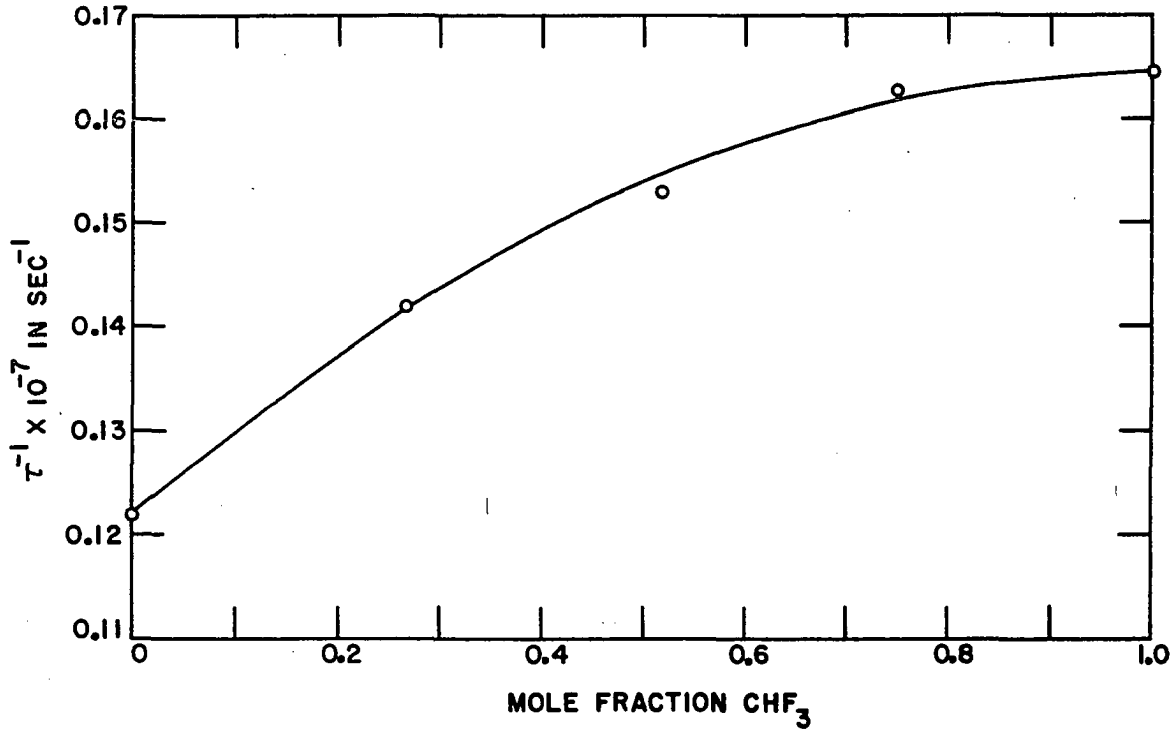

Fig. 45 Reciprocal relaxation time vs. concentration in CHF_3 - CF_4 mixtures.

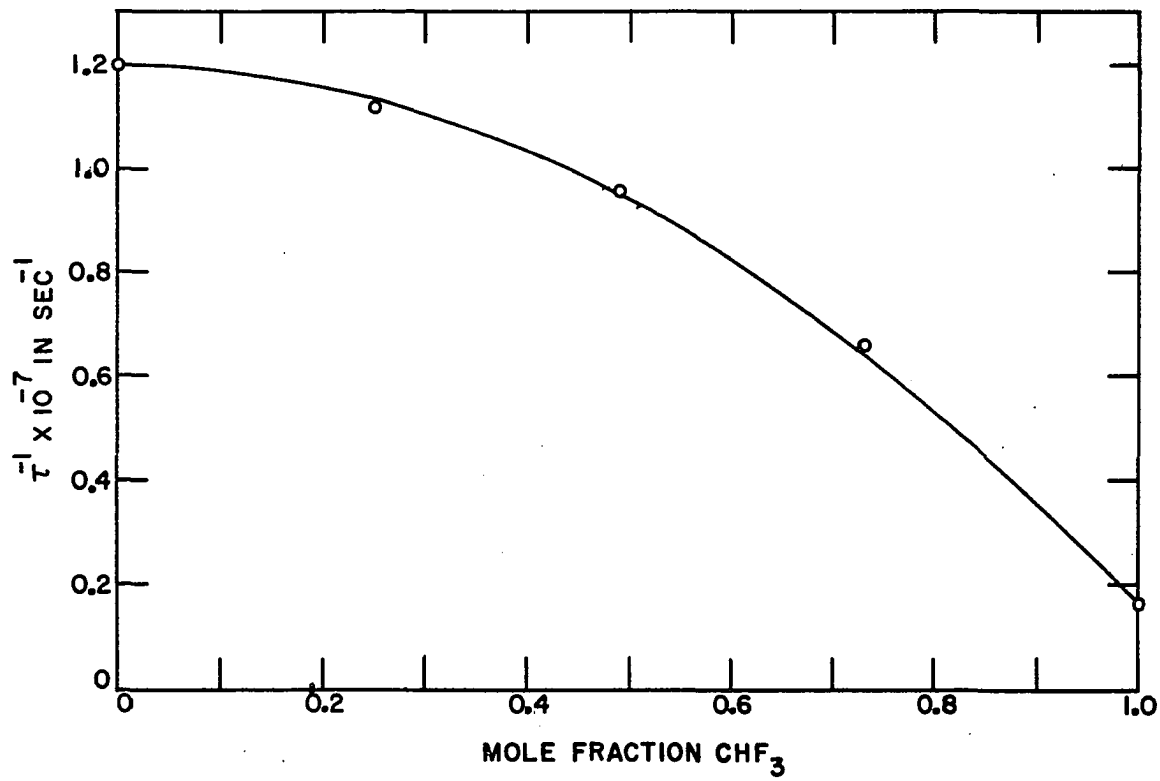

Fig. 46 Reciprocal relaxation time vs. concentration in CHF_3 - CCl_2F_2 mixtures.

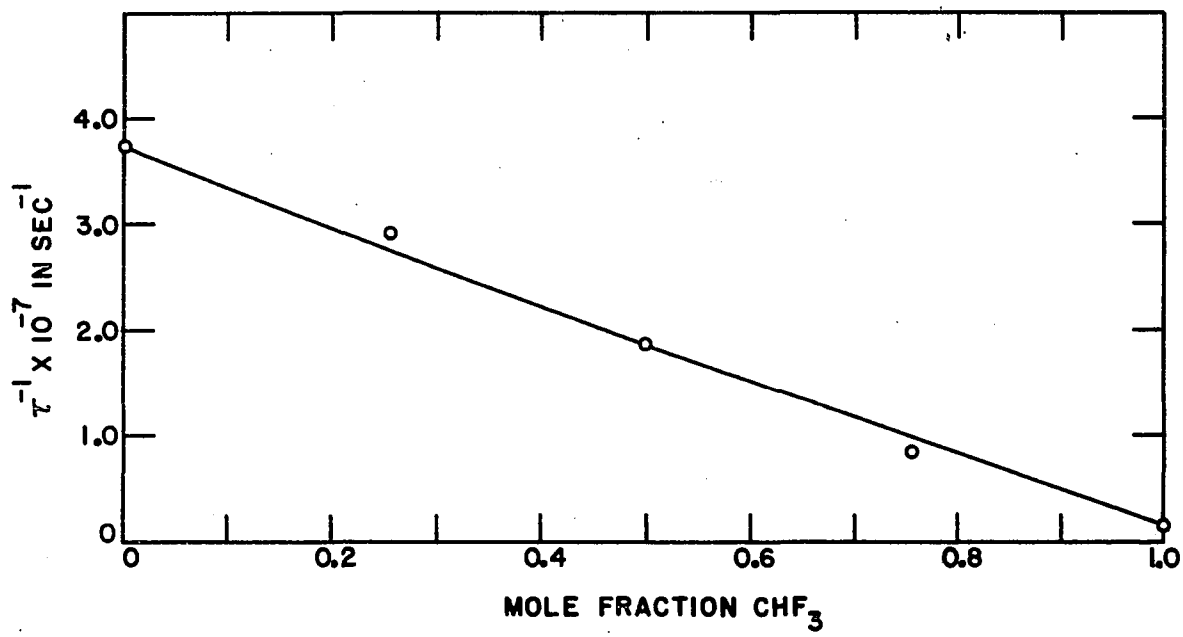

Fig. 47 Reciprocal relaxation time vs. concentration in CHF_3 - $CHCl_2F$ mixtures.

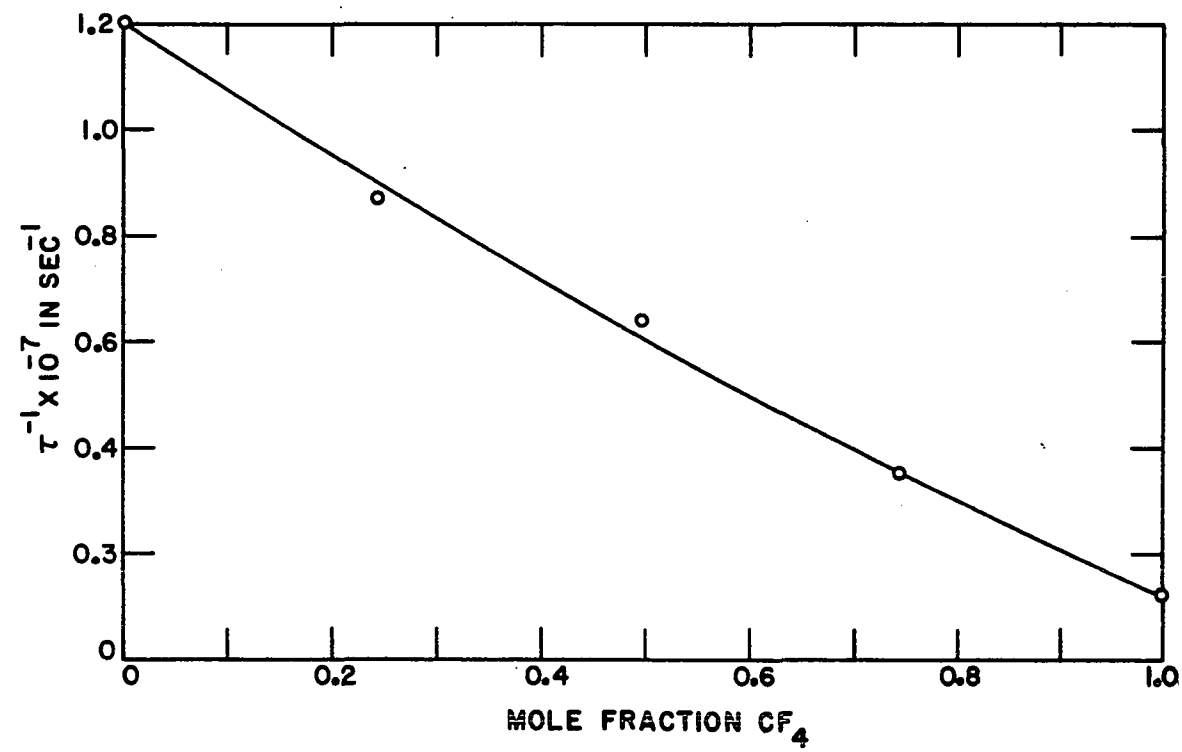

Fig. 48 Reciprocal relaxation time vs. concentration in CF_4 - CCl_2F_2 mixtures.

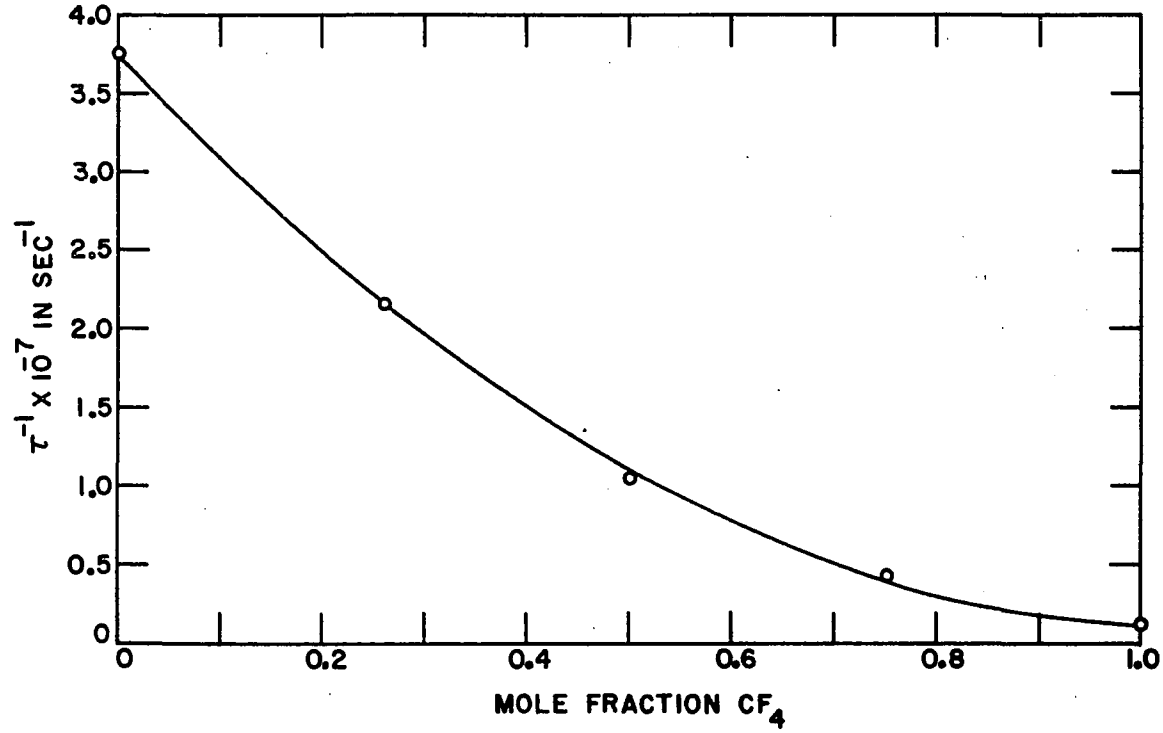

Fig. 49 Reciprocal relaxation time vs. concentration in CF_4 - $CHCl_2F$ mixtures.

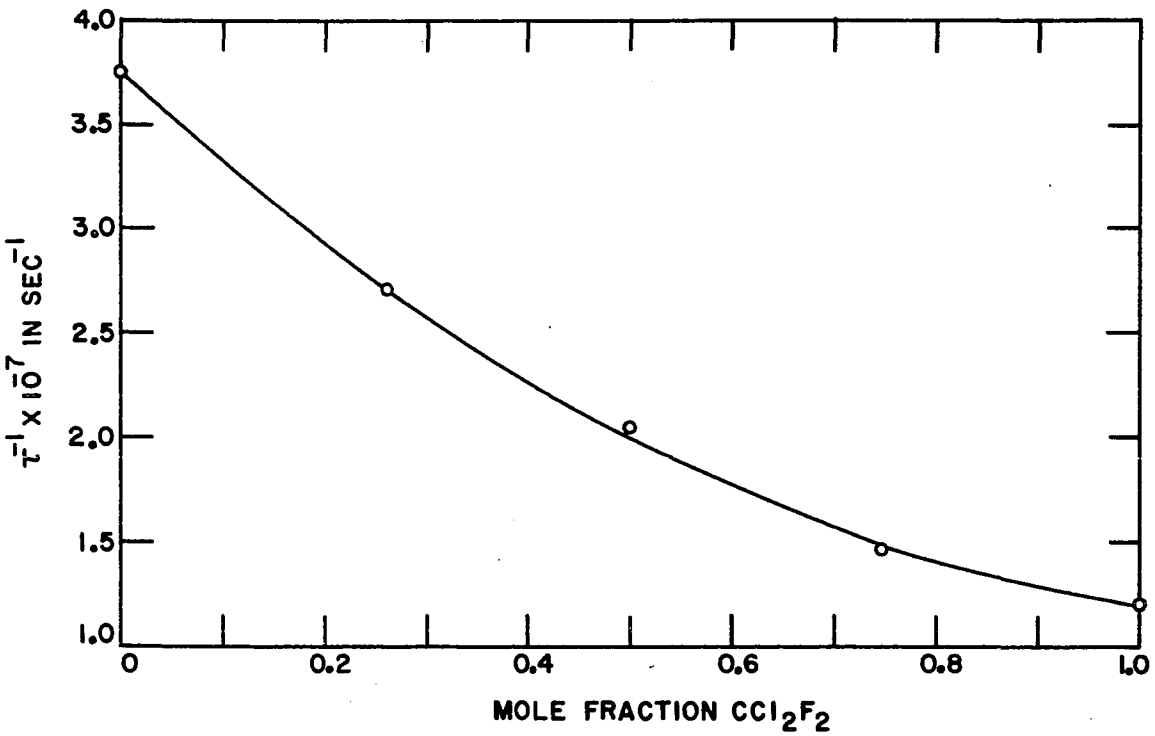

Fig. 50 Reciprocal relaxation time vs. concentration in CCl_2F_2 - $CHCl_2F$ mixtures.

relaxation time on concentration can be verified by comparing the values of $(\tau_{AB}^{-1} + \tau_{BA}^{-1})$ obtained for the various concentrations. If Equation 59 is valid, the values of this quantity should be independent of concentration. As was indicated earlier, Equation 59 should be valid if the individual relaxation times of the mixture components are similar and if their vibrational specific heats are similar. Values of $(\tau_{AB}^{-1} + \tau_{BA}^{-1})$ for mixtures which come closest to satisfying the above requirements are given in Table 4. The agreement here is very good; certainly within the limits of experimental error. Values of $(\tau_{AB}^{-1} + \tau_{BA}^{-1})$ for mixtures not satisfying the requirements are given in Table 5. The agreement here is, in general, poor. The notable examples are the CH_2F_2-CF_4 mixtures. The values of $(\tau_{AB}^{-1} + \tau_{BA}^{-1})$ for these mixtures were, for the most part, meaningless. A number of runs were made at various concentrations. These yielded values ranging from small positive numbers to negative numbers. The negative numbers, of course, have no meaning as relaxation times.

B. Theoretical

Theoretical values of τ_{AB}^{-1} and τ_{BA}^{-1} have been calculated from Equation 93. In order to make these calculations, values for the various parameters in the equation must be

determined for each gas and each mixture.

If we assume the parameters, ϵ and r_o, in Equation 83 are similar to those in Equation 78, we can follow the methods of Hirschfelder *et al.* (13) to determine their values. ϵ is approximately given by the relation, $\epsilon = kT_c/1.28$. r_o is estimated by comparing the second viral coefficient obtained from Equation 22 with that obtained from

$$B = \frac{2}{3} N r_o^3 \sum_{j=0}^{\infty} b_j T^{*-(2j+1)/4} , \qquad \text{(Eq. 95)}$$

where

$$T^* = \frac{kT}{\epsilon} ,$$

$$b_j = - \frac{2^{j+\frac{1}{2}}}{4j!} \Gamma\left(\frac{2j-1}{4}\right) ,$$

and N is Avogodro's number. Values of b_j are tabulated in Table I-E of the appendix of Reference 13.

The parameter, s, can be obtained from Figure 1 after the values of E_m and ϵ are determined. For mixtures, r_o^{AB}, ϵ_{AB}, and s_{AB} can be estimated from $r_o^{AB} = \frac{1}{2}(r_o^A + r_o^B)$, $\epsilon_{AB} = (\epsilon_A \epsilon_B)^{\frac{1}{2}}$, and $s_{AB} = \frac{1}{2}(s_A + s_B)$, respectively.

$\tilde{R}$ can be calculated from the Sutherland equation (13),

$$\tilde{R} = \sqrt{2}\, n\pi r_o^2 \bar{v}(1 + S/T) . \qquad \text{(Eq. 96)}$$

Here n is the density of molecules, $\bar{v}$ is the mean thermal speed of the molecules, given by $\bar{v} = (8RT/M\pi)^{\frac{1}{2}}$, and S is the Sutherland constant, given by $S \cong 0.8T_c$. For mixtures, $\tilde{R}_{AB}$ is given by (7)

$$\tilde{R}_{AB} = n_B(r_o^{AB})^2(\bar{v}_A^2 + \bar{v}_B^2)^{\frac{1}{2}}(1 + S_{AB}/T) \ , \qquad \text{(Eq. 97)}$$

where $S_{AB} \cong (S_A S_B)^{\frac{1}{2}}$. Since the $\tilde{R}$'s appear in Equation 93 as a ratio, the calculation can be simplified by combining Equations 96 and 97. The ratio then is

$$\frac{\tilde{R}_{AB}}{\tilde{R}_A} = \frac{1}{4\sqrt{2}} (1 + r_o^B/r_o^A)^2(1 + M_A/M_B)^{\frac{1}{2}} \frac{(1 + S_{AB}/T)}{(1 + S_A/T)} \ . \qquad \text{(Eq. 98)}$$

Other terms appearing in Equation 93 as ratios can also be simplified. These are the following:

$$\frac{\theta'_{AB}}{\theta'_A} = \tfrac{1}{2}(1 + M_A/M_B)^{-1}(1 + s_B/s_A)^2 \qquad \text{(Eq. 99)}$$

and

$$\frac{Y_A}{Y_{AB}} = (1 + 1.1\epsilon_A/kT)(1 + 1.1\epsilon_{AB}/kT)^{-1} \ . \qquad \text{(Eq. 100)}$$

The terms involving θ'_A and θ'_{AB} in the exponent can be re-written as

$$\frac{3}{2}(\theta'_A/T)^{1/3}[1 - (\theta'_{AB}/\theta'_A)^{1/3}] . \qquad \text{(Eq. 101)}$$

Values of the pure gas parameters pertinent to the calculations are given in Table 6. Table 7 contains values for various quantities appearing in Equation 93. The temperature dependent terms in these tables have been calculated at 298°K. This temperature is about the average temperature at which the experimental data were taken.

The theoretical values of τ_{AB}^{-1} and τ_{AB}^{-1} are very sensitive to small changes in the exponent, particularly if the exponent is large. Since the dominant terms in the exponent are those containing the (θ')'s, small variations in these quantities will have a large effect on the values of the τ's. The parameters upon which θ' depends are all fairly well established, with the exception of the range of interaction, s. The ratio, r_o/s, depends strongly on the steepness of the repulsive part of the potential existing between the interacting molecules. If the values of r_o are close to correct, comparison of the experimental and theoretical values of $(\tau_{AB}^{-1} + \tau_{BA}^{-1})$ can yield information concerning the accuracy of the assumed repulsive potential.

The results of the theoretical calculations appear in Table 8 along with the experimental values of $(\tau_{AB}^{-1} + \tau_{BA}^{-1})$. The experimental values given here are the average of

Table 6. Values of various pure gas parameters (temperature dependent quantities determined at 298°K)

Gas	P_c (atm)	T_c (°K)	$r_o(10^8)$ cm	ϵ/kT	E_m/ϵ	r_o/s	$s(10^8)$ cm	θ'/T
CH_2F_2	71.3	374	4.36	.981	1.201	39.1	.111	517
CHF_3	56.5	323	4.38	.847	1.503	38.5	.114	663
CF_4	36.9	228	4.20	.598	2.063	37.6	.112	595
CCl_2F_2	39.6	385	5.37	1.009	1.098	39.4	.136	431
$CHCl_2F$	51.0	452	5.34	1.184	.906	40.0	.134	391

those given in Tables 4 and 5. The first group of values in Table 8 correspond to the mixtures for which the requirements of Equation 59 are met. The second group are those for which the requirements are not met.

In general, the agreement between the experimental and theoretical values in the first group is quite good. Little can be said for the agreement in the second group, since the experimental values are of questionable merit. In comparing the experimental and theoretical values, one must consider the approximations made in the theoretical calculations.

First, Equation 93 has been derived for a diatomic vibrating molecule. The molecules discussed here are more

Table 7. Values for various quantities required for calculation of τ_{AB}^{-1} and τ_{BA}^{-1}

Gas A	Gas B	$\frac{\tilde{R}_{AB}}{\tilde{R}_A}$	$\frac{Y_A}{Y_{AB}}$	$(\frac{\theta'_{AB}}{\theta'_A})^{\frac{7}{6}}$	$\frac{3}{2}[(\frac{\theta'_A}{T})^{\frac{1}{3}} - (\frac{\theta'_{AB}}{T})^{\frac{1}{3}}]$	$\frac{\epsilon_{AB} - \epsilon_A}{kT}$
CH_2F_2	CHF_3	.904	1.038	1.204	-.655	-.069
CH_2F_2	CF_4	.869	1.128	1.311	-.969	-.215
CH_2F_2	CCl_2F_2	1.062	.993	1.895	-2.413	+.014
CH_2F_2	$CHCl_2F$	1.128	.951	1.740	-2.065	+.097
CHF_3	CF_4	.843	1.084	1.111	-.399	-.135
CHF_3	CCl_2F_2	1.147	.958	1.656	-2.027	+.077
CHF_3	$CHCl_2F$	1.226	.919	1.490	-1.578	+.155
CF_4	CCl_2F_2	1.343	.894	1.513	-1.584	+.179
CF_4	$CHCl_2F$	1.434	.861	1.358	-1.152	+.244
CCl_2F_2	$CHCl_2F$	1.080	.958	.886	+ .385	+.084

Gas A	Gas B	$\frac{\tilde{R}_{BA}}{\tilde{R}_B}$	$\frac{Y_B}{Y_{BA}}$	$(\frac{\theta'_{BA}}{\theta'_B})^{\frac{7}{6}}$	$\frac{3}{2}[(\frac{\theta'_B}{T})^{\frac{1}{3}} - (\frac{\theta'_{BA}}{T})^{\frac{1}{3}}]$	$\frac{\epsilon_{BA} - \epsilon_B}{kT}$
CH_2F_2	CHF_3	1.116	.965	.810	+.765	+.064
CH_2F_2	CF_4	1.331	.900	.704	+1.203	+.168
CH_2F_2	CCl_2F_2	1.049	1.007	.442	+2.358	-.014
CH_2F_2	$CHCl_2F$	.956	1.054	.513	+1.905	-.107
CHF_3	CF_4	1.186	.930	.887	+ .426	+.114
CHF_3	CCl_2F_2	.920	1.046	.569	+1.684	-.084
CHF_3	$CHCl_2F$	.841	1.096	.653	+1.259	-.183
CF_4	CCl_2F_2	.764	1.138	.657	+1.282	-.232
CF_4	$CHCl_2F$	.699	1.196	.745	+ .884	-.343
CCl_2F_2	$CHCl_2F$	.927	1.046	1.120	- .362	-.091

Table 8. Values of τ_{AB}^{-1}, τ_{BA}^{-1}, and $(\tau_{AB}^{-1} + \tau_{BA}^{-1})$

Gas A	Gas B	$\tau_{AB}^{-1}(10^{-7})$ (sec^{-1}) (theo.)	$\tau_{BA}^{-1}(10^{-7})$ (sec^{-1}) (theo.)	$(\tau_{AB}^{-1} + \tau_{BA}^{-1})(10^{-7})$ (sec^{-1}) (theo.)	$(\tau_{AB}^{-1} + \tau_{BA}^{-1})(10^{-7})$ (sec^{-1}) (expt'l.)
CH_2F_2	CCl_2F_2	.636	3.52	4.16	5.56
CH_2F_2	$CHCl_2F$	.868	7.85	8.72	20.1
CHF_3	CF_4	.109	.181	.290	.329
CHF_3	CCl_2F_2	.0539	2.39	2.44	2.40
CF_4	CCl_2F_2	.0629	1.65	1.71	1.09
CCl_2F_2	$CHCl_2F$	1.62	2.79	4.41	3.03
CH_2F_2	CHF_3	1.58	.280	1.86	1.10
CH_2F_2	CF_4	1.24	.301	1.54	-
CHF_3	$CHCl_2F$	.0792	5.35	5.43	3.55
CF_4	$CHCl_2F$	.0889	3.70	3.79	.563

complex than diatomic molecules and a more rigorous derivation probably would be valuable. However, since only the lowest vibrational mode contributes to the exchange of energy and these variations are assumed to be spherically symmetric, the application of Equation 93 to complex molecules can be made without serious loss of generality.

The assumption that the quantity, Z_o, is the same for both A-B and A-A collisions may not be true. This term is a geometric factor, related to the probability that the colliding molecules will be oriented in such a way as to make an energy transfer possible. Since the A and B molecules differ geometrically, the values of Z_o could be different for the two types of collisions. Errors could also be introduced because of the assumption that $(r_o^{AB}/r_c^{AB}) \simeq (r_o^A/r_o^A)$. These errors should, however, be small. Of greater concern are the parameters pertinent to interactions involving unlike molecules, i.e. s_{AB}, ϵ_{AB}, etc. The methods used to determine these quantities are, in general, empirical and result in only approximate values.

Considering the various approximations made in the derivation of Equation 93 and the other approximations necessary for the calculation of theoretical values of the τ's, the agreement between the experimental and theoretical values of $(\tau_{AB}^{-1} + \tau_{BA}^{-1})$ must be considered good. This statement, of course, applies only to those mixtures for which

the requirements of Equation 59 are satisfied. Analysis of Table 8 does not indicate that an overall change in the steepness of the repulsive potential would be warranted. In some cases better agreement would result with a larger value of s, but other cases would require a smaller value. Thus, the conclusion is that, for molecules of this type, a Lennard-Jones type potential with a repulsive part proportional to r^{-28} is reasonable.

V. CONCLUSIONS

On the basis of the work reported here, the following conclusions can be drawn:

1. A single relaxation time seems to exist in the mixtures discussed here. No real evidence of multiple dispersion was observed, although the CHF_3-$CHCl_2F$ and CF_4-$CHCl_2F$ mixtures do not follow the single dispersion curves as well as the other mixtures.

2. The quadratic dependence of the observed relaxation times of the mixtures on concentration appears to be valid when the relaxation times of the individual gases are similar and when the vibrational specific heats of the gases are similar. How similar these quantities must be is not well defined, but it would appear that if the relaxation times are of the same order of magnitude, and the specific heats differ by less than a factor of 3, the quadratic equation is valid.

3. Judging from the agreement between the experimental and theoretical values for $(\tau_{AB}^{-1} + \tau_{BA}^{-1})$, a Lennard-Jones interaction potential with a repulsive part proportional to r^{-28} is close to correct for halomethane gases.

VI. BIBLIOGRAPHY

1. Amme, R. C. and Legvold, S. Sound dispersion in halo-methane mixtures. Journal of Chemical Physics 26, 514 (1956).

2. Amme, R. C. and Legvold, S. Temperature dependence of sound dispersion in halo-methane gases. Journal of Chemical Physics 30, 163 (1959).

3. Amme, R. C. and Legvold, S. Vibrational transitions and the intermolecular potential. Journal of Chemical Physics 33, 91 (1960).

4. Bradley, C. A., Jr. Raman spectra of $SiHCl_3$, $CHFCl_2$, and CF_2Cl_2. Physical Review 40, 908 (1932).

5. Calvert, J. B. and Amme, R. C. Multiple velocity dispersion in halo-methane gas mixtures. Journal of Chemical Physics 33, 1270 (1960).

6. de Wette, F. W. and Slawsky, Z. I. Influence of adiabatic interactions on the energy transfer in molecular collisions. Physica 20, 1169 (1954).

7. Euchen, A. and Becker, R. Die Stossanregung intramolekularer Schwingungen in Gasen und Gasmischungen auf Grund von Schalldispersionsmessungen. II. Die Schalldispersion bei verschiedenen Temperaturen in Chlor und Kohlendioxyd (rein und mit Fremdgaszusätzen). Zeitschrift für Physikalische Chemie B27, 235 (1934).

8. Fogg, P. G. T., Hanks, P. A. and Lambert, J. D. Ultrasonic dispersion in halo-methane vapours. Royal Society of London, Proceedings A219, 490 (1953).

9. Glockler, G. and Leader, G. R. The fundamental frequencies of certain trihalomethanes. Journal of Chemical Physics 8, 699 (1940).

10. Hamann, S. D. and Lambert, J. A. The behavior of quasispherical molecules. I. Gases at low densities. Australian Journal of Chemistry 7, 1 (1954).

11. Herzberg, G. Molecular spectra and molecular structure. New York, D. Van Nostrand Company, Inc. (1945).

12. Herzfeld, K. E. and Litovitz, T. A. Absorption and dispersion of ultrasonic waves. Pure and Applied Physics 7, 1 (1959).

13. Hirschfelder, J. O., Curtiss, C. F. and Bird, R. B. Molecular theory of gases and liquids. New York, John Wiley and Sons, Inc. (1954).

14. Jackson, J. M. and Mott, N. F. The energy exchange between inert gas atoms and a solid surface. Royal Society of London, Proceedings A137, 703 (1932).

15. Kallmann, H. and London, P. Über quanten-mechanische Energieubertraguing zwischen atomaren systemen. Zeitschrift für Physikalische Chemie B2, 207 (1929).

16. Kennard, E. H. Kinetic theory of gases. New York, McGraw-Hill Book Company, Inc. (1938).

17. Landau, L. and Teller, E. Zur theory der Schalldispersion. Physikalische Zeitschrift der Sowjetunion 10, 34 (1936).

18. McCourbrey, J. C., Milward, R. C. and Ubbelohde, A. R. Transition probabilities for the transfer of vibrational energy. Faraday Society Transactions 57, 1472 (1961).

19. Miyahara, Y. and Richardson, E. G. Ultrasonic relaxation in freon vapors. The Acoustic Society of America Journal 28, 1016 (1956).

20. Olson, J. R. Sound dispersion in substituted methane-inert gas mixtures. Unpublished Ph.D. thesis. Ames, Iowa, Library, Iowa State University of Science and Technology (1963).

21. Olson, J. R. and Legvold, S. Sound dispersion in substituted methane-inert gas mixtures. Journal of Chemical Physics 39, (1963).

22. Pierce, G. W. Piezoelectric crystal oscillator applied to precision measurements of the velocity of sound in air and CO_2 at high frequencies. American Academy of Arts and Sciences Proceedings 60, 271 (1925).

23. Rank, D. H. and Shull, E. R. Vibrational spectra of some fluoromethanes. Journal of Chemical Physics 18, 885 (1950).

24. Reed, T. M., III. The theoretical energies of mixing for fluorocarbon-hydrocarbon mixtures. Journal of Chemical Physics 59, 425 (1955).

25. Rice, O. K. On collision problems involving large interactions. Physical Review 38, 1943 (1931).

26. Richards, W. T. Supersonic phenomena. Review of Modern Physics 11, 36 (1939).

27. Rossing, T. D. and Legvold, S. Collision excitation of molecular vibrations in halogen-substituted methanes. Journal of Chemical Physics 23, 1118 (1955).

28. Rossing, T. D. Oscillator for acoustic interferometry. Unpublished M.S. thesis. Ames, Iowa, Library, Iowa State University of Science and Technology (1952).

29. Rossing, T. D. Sound dispersion in halogen-substituted methanes. Unpublished Ph.D. thesis. Ames, Iowa, Library, Iowa State University of Science and Technology (1954).

30. Schwartz, R. N. and Herzfeld, K. F. Vibrational relaxation times in gases (three-dimensional treatment). Journal of Chemical Physics 22, 767 (1954).

31. Schwartz, R. N., Slawsky, Z. I. and Herzfeld, K. F. Calculation of vibrational relaxation times in gases. Journal of Chemical Physics 20, 1591 (1952).

32. Sette, C., Busala, A. and Hubbard, J. C. Energy transfer by collision in vapors of clorinated methanes. Journal of Chemical Physics 23, 787 (1955).

33. Tanczos, F. I. Calculation of vibrational relaxation times in the cloromethanes. Journal of Chemical Physics 25, 439 (1956).

34. Valley, L. M. and Legvold, S. Sound dispersion in ethane and 1.1-difluoroethane. Journal of Chemical Physics 33, 627 (1960).

35. Valley, L. M. and Legvold, S. Vibrational relaxation times for gas mixtures. Physics of Fluids 3, 931 (1960).

36. Zener, C. Low velocity inelastic collisions. Physical Review 38, 277 (1931).

37. Zener, C. Some observations on the theory of interchange of vibrational and translational energy. Cambridge Philosophical Society Proceedings 29, 136 (1933).

VII. ACKNOWLEDGMENTS

The author wishes to express his sincere gratitude to Dr. Sam Legvold for his patience and guidance during the course of this investigation.

The gases used in this study were provided by the Jackson Laboratories of the E. I. du Pont de Nemours and Company. The author wishes to express his appreciation for this contribution.

Thanks are also due to the Air Force Office of Scientific Research whose financial support made this work possible.